Development 140, 433-443 (2013) doi:10.1242/dev.083949

Regulation of cytoskeletal organization and junctional remodeling by the atypical cadherin Fat

Emily Marcinkevicius[1,2] and Jennifer A. Zallen[1,*]

SUMMARY

The atypical cadherin Fat is a conserved regulator of planar cell polarity, but the mechanisms by which Fat controls cell shape and tissue structure are not well understood. Here, we show that Fat is required for the planar polarized organization of actin denticle precursors, adherens junction proteins and microtubules in the epidermis of the late *Drosophila* embryo. In wild-type embryos, spatially regulated cell-shape changes and rearrangements organize cells into highly aligned columns. Junctional remodeling is suppressed at dorsal and ventral cell boundaries, where adherens junction proteins accumulate. By contrast, adherens junction proteins fail to accumulate to the wild-type extent and all cell boundaries are equally engaged in junctional remodeling in *fat* mutants. The effects of loss of Fat on cell shape and junctional localization, but not its role in denticle organization, are recapitulated by mutations in Expanded, an upstream regulator of the conserved Hippo pathway, and mutations in Hippo and Warts, two kinases in the Hippo kinase cascade. However, the cell shape and planar polarity defects in *fat* mutants are not suppressed by removing the transcriptional co-activator Yorkie, suggesting that these roles of Fat are independent of Yorkie-mediated transcription. The effects of Fat on cell shape, junctional remodeling and microtubule localization are recapitulated by expression of activated Notch. These results demonstrate that cell shape, junctional localization and cytoskeletal planar polarity in the *Drosophila* embryo are regulated by a common signal provided by the atypical cadherin Fat and suggest that Fat influences tissue organization through its role in polarized junctional remodeling.

KEY WORDS: *Drosophila*, Fat, Actin, Cell adhesion, Microtubules, Planar polarity

INTRODUCTION

Epithelial cell polarity plays an essential role in tissue structure. In addition to apical and basolateral domains, many epithelia display asymmetries in the plane of the tissue, referred to as planar cell polarity (Zallen, 2007; Goodrich and Strutt, 2011; Gray et al., 2011). Planar asymmetries can generate directional fluid flow (Marshall and Kintner, 2008; Wallingford, 2010), multicellular structures that mediate hearing and vision (Kelly and Chen, 2009; Wu and Mlodzik, 2009) and left-right asymmetry of the body plan (Goetz and Anderson, 2010; Hashimoto and Hamada, 2010). The atypical cadherins Fat and Dachsous regulate the planar-polarized orientation of hairs, bristles and ommatidia in *Drosophila* and organize cell movements and cell-shape changes that influence tissue structure (Thomas and Strutt, 2012). Fat and Dachsous regulate cell shape, rearrangement and oriented divisions during tissue elongation in the *Drosophila* wing (Baena-López et al., 2005; Aigouy et al., 2010), and mammalian Fat4 and Dachsous 1 are required for elongation of the neural tube, cochlea, kidney and intestines (Saburi et al., 2008; Saburi et al., 2012; Mao et al., 2011a). However, the cellular and molecular mechanisms by which these conserved planar polarity regulators influence cell shape and tissue organization are not well understood.

The *Drosophila* embryo displays a striking planar organization. Groups of cells in the ventral epidermis generate actin- and microtubule-based protrusions that initiate at the posterior cell cortex and provide a template for denticles in the larval cuticle that point in an anterior or posterior direction (Bate and Martinez-Arias, 1993; Dickinson and Thatcher, 1997). In addition, denticle-forming cells elongate along the dorsal-ventral axis and align their anterior and posterior borders (Price et al., 2006; Walters et al., 2006; Simone and DiNardo, 2010), producing highly aligned columns of cells. These structures resemble compartment boundaries and tissue-level patterns in the vertebrate retina (Major and Irvine, 2006; Landsberg et al., 2009; Monier et al., 2010; Salbreux et al., 2012). Planar-polarized cell behaviors in the denticle field are accompanied by an asymmetric localization of cytoskeletal and junctional proteins, including the nonmuscle myosin II motor protein, which is enriched at borders between anterior and posterior cells and is necessary for cell shape (Walters et al., 2006; Simone and DiNardo, 2010). Adherens junction proteins accumulate at the complementary borders between dorsal and ventral cells, although the function of this localized enrichment is not known (Colosimo and Tolwinski, 2006; Price et al., 2006; Kaplan and Tolwinski, 2010; Simone and DiNardo, 2010). It is not clear whether different manifestations of planar polarity in the denticle field are generated independently or if they occur in response to a common upstream signal.

Although the Frizzled planar polarity pathway plays a minor role in denticle organization (Price et al., 2006), Fat and Dachsous are essential for this process (Casal et al., 2006; Repiso et al., 2010; Donoughe and DiNardo, 2011). Dachsous (Ds) binds heterophilically to Fat (Strutt and Strutt, 2002; Ma et al., 2003; Matakatsu and Blair, 2004; Matakatsu and Blair, 2006), and Ds and the kinase Four-jointed are expressed in gradients in several tissues and are proposed to generate a graded pattern of Fat signaling (Zeidler et al., 1999; Zeidler et al., 2000; Casal et al., 2002; Yang et al., 2002; Ma et al., 2003; Simon, 2004). Ds is highly expressed in the posterior half of the denticle field, and misexpression causes denticles to reorient toward sites of ectopic Ds (Repiso et al., 2010;

[1]Howard Hughes Medical Institute and Developmental Biology Program, Sloan-Kettering Institute, 1275 York Avenue, New York, NY 10065, USA. [2]Weill Cornell Graduate School of Medical Sciences, Cornell University, 1300 York Avenue, New York, NY 10065, USA.

*Author for correspondence (zallenj@mskcc.org)

Accepted 8 November 2012

Donoughe and DiNardo, 2011). Despite substantial progress in understanding the upstream signals that regulate Fat activity, the cellular and molecular mechanisms by which Fat controls planar tissue organization are not well understood.

Fat and Ds are asymmetrically localized within cells (Ambegaonkar et al., 2012; Bosveld et al., 2012; Brittle et al., 2012) and could influence cell polarity directly or through the regulation of downstream effectors. However, the relationship between these molecular asymmetries and the asymmetric shapes and behaviors of cells is not clear. Fat and Ds regulate the localization and activity of Frizzled pathway proteins (Adler et al., 1998; Strutt and Strutt, 2002; Yang et al., 2002; Ma et al., 2003), but some effects of Fat and Ds are independent of Frizzled (Casal et al., 2006; Donoughe and DiNardo, 2011). Fat/Ds signaling produces an asymmetric localization of the unconventional myosin Dachs, which is required for cell and tissue shape (Mao et al., 2006; Rogulja et al., 2008; Mao et al., 2011b; Bosveld et al., 2012). Fat binds to Atrophin (Grunge – FlyBase), a transcriptional regulator that is required for planar polarity in the eye (Zhang et al., 2002; Fanto et al., 2003; Saburi et al., 2012). Ds regulates microtubule organization in the wing and has been proposed to influence microtubule-dependent protein transport (Shimada et al., 2006; Harumoto et al., 2010). Fat and Ds also regulate cell growth and survival by activating the Hippo-Warts kinase cascade (Bryant et al., 1988; Bennett and Harvey, 2006; Cho et al., 2006; Silva et al., 2006; Willecke et al., 2006; Tyler and Baker, 2007). However, the role of Fat in growth regulation requires different sequences in the Fat cytoplasmic domain (Matakatsu and Blair, 2012), and is generally considered to be separate from its role in planar polarity.

Here, we show that Fat is required for the planar polarized organization of denticle actin precursors, adherens junction proteins and microtubules in the *Drosophila* embryo. These defects are associated with a disruption of cell shape and polarized junctional remodeling in *fat* mutants. The effects of loss of Fat on cell shape and adherens junction localization, but not its role in denticle planar polarity, are recapitulated by mutations in the FERM-domain protein Expanded, a regulator of the Hippo pathway, and in Hippo and Warts, two kinases in the Hippo kinase cascade, but these effects do not require transcriptional regulation by Yorkie. Similar defects in cell shape, microtubule organization and junctional localization and remodeling occur in embryos that express activated Notch. These results demonstrate that junctional and cytoskeletal planar polarity are regulated by a common upstream signal provided by the atypical cadherin Fat, and suggest that Fat could influence cell shape and tissue organization through its role in polarized junctional remodeling.

MATERIALS AND METHODS

Fly stocks and genetics

Embryos were generated at room temperature (21-23°C). Alleles were *fat*^{NY1} (Tyler et al., 2007), *fat*^{Grv} (Bryant et al., 1988), *ds*^{UAO71} (Adler et al., 1998), *fz*^{R52} (Adler et al., 1994), *vang*^{A3} (Taylor et al., 1998), *ex*^{E1} (Boedigheimer and Laughon, 1993), *ex*^{MGH1} (Pellock et al., 2007), *hpo*^{MGH1}, *hpo*^{MGH2} (Harvey et al., 2003), *yki*^{B5} (Huang et al., 2005), *wts*^{X1} (Xu et al., 1995), *d*^{GC13} (Mao et al., 2006), Su(H)*lacZ* (Go et al., 1998) and *fj:GFP* (flytrap.med.yale.edu). Embryos expressing UAS-*yki*^{S168A} (Oh and Irvine, 2008), UAS-*N*^{intra} (Struhl and Adachi, 1998) or UAS-*dachs:V5* (Mao et al., 2006) were the progeny of da-Gal4 females × UAS males. Germline clones were generated with the FLP-DFS system (Chou and Perrimon, 1996) using *ovo*^{D2} FRT40A, FRT42D *ovo*^{D1} (gift of G. Struhl, Columbia University), or FRT82B *ovo*^{D2}. Homozygous mutant embryos were identified by the absence of GFP from twi-*Gal4*, UAS-*GFP* balancers in embryos sorted prior to fixation on a Leica MZFLII microscope.

To generate the *fat*^{NY1} *yki*$^{B5\ m/z}$ double mutant, larvae of the genotype hs-flp/+; *fat*^{NY1} FRT42D *yki*^{B5}/FRT42D *ovo*^{D1} were heat shocked and crossed to *fat*^{NY1} FRT42D *yki*^{B5}/CyO, twi-Gal4, UAS-GFP males and GFP(–) embryos selected as above. All GFP(–) embryos were maternally and zygotically mutant for *yki*^{B5} and half are predicted to be zygotically mutant for *fat*^{NY1} (8/13 stage 14 embryos had cell shape and junctional localization defects similar to *fat*^{NY1}).

Immunohistochemistry

For antibodies to Arm (β-catenin), Pyd (ZO-1), Baz (Par-3) and Ex, embryos were boiled for 10 seconds in 0.03% Triton X-100 and 0.4% NaCl, cooled for 30 minutes on ice and devitellinized in heptane:methanol (1:1). For GFP, phalloidin, Yki, V5 and E-cadherin (Shotgun – FlyBase), embryos were fixed for 1 hour in 5.5% formaldehyde in 0.1 M $NaPO_4$, pH 7.2, and manually devitellinized. For α-tubulin and E-cadherin co-staining, embryos were fixed for 10 minutes in 33% formaldehyde with 50 mM EGTA in 0.1 M $NaPO_4$, pH 7.2, and manually devitellinized. Antibodies were mouse anti-β-catenin [1:50, Developmental Studies Hybridoma Bank (DSHB)], guinea pig anti-Pyd (1:500) (Wei and Ellis, 2001), rabbit anti-Baz (1:500) (Blankenship et al., 2006), guinea pig anti-Ex (1:500) (Maitra et al., 2006), rabbit anti-GFP (1:1000, Torrey Pines), rabbit anti-Yki (1:200) (Oh and Irvine, 2008), mouse anti-V5 (1:50, Molecular Probes), rat anti-E-cadherin (1:25, DSHB) and mouse anti-α-tubulin (1:500, Sigma). Secondary antibodies conjugated to Alexa Fluor 488, Alexa Fluor 568 and Alexa Fluor 647 (Molecular Probes) were used at 1:500. Alexa Fluor 488-conjugated phalloidin was used at 1:1000 (Molecular Probes). Embryos were mounted in Prolong Gold with DAPI (Molecular Probes) and imaged on a Zeiss LSM510 META confocal microscope with a PlanNeo 40×/1.3NA objective. *z*-slices (1.0 μm thick) were acquired at 0.5 μm steps. Maximum intensity projections of *z*-slices spanning 2-3 μm in the region of the adherens junctions were analyzed.

Time-lapse imaging

Time-lapse imaging was performed on embryos expressing β-catenin:GFP from the endogenous promoter (McCartney et al., 2001). Embryos were dechorionated in 50% bleach, mounted on a YSI membrane with halocarbon oil 27 (Sigma), and imaged on a Perkin Elmer RS5 spinning disk confocal microscope with a Zeiss PlanApo 63×/1.4NA objective. *z*-stacks were acquired every 30 seconds at *z*-slices 1.0 μm apart. Edge growth and contraction were analyzed manually by following all events in which an edge contracted to a vertex and subsequently resolved into an edge. Cells were analyzed from the fusion of the ventral midline at stage 13 until muscle contraction at stage 16 (~2.5 hours).

Measurements and statistics

Analysis was of segments A2-A7. Embryos were staged by the extent of germband retraction (stage 12), the morphology of the amnioserosa/epidermal border (stage 13), the extent of dorsal closure (stage 14) and the extent of gut constriction (stage 16). For denticle placement, precursors that contacted only the anterior or posterior cell boundary were scored as anteriorly or posteriorly localized, respectively. Precursors that contacted neither boundary were considered to be centrally localized. Precursors that contacted both cell boundaries (in very narrow cells) were not analyzed. Oregon R was the wild-type control.

Edge alignment was analyzed as described (Simone and DiNardo, 2010). Denticle columns were identified by their position relative to sensory organ precursors, which are located two columns anterior to denticle column 1. In addition, the column 1/2 and 4/5 boundaries are more aligned and depleted of junctional proteins and column 6 cells have a distinct narrow, highly elongated morphology that marks the posterior edge of the denticle field. Angles between adjacent anterior-posterior (AP) edges were converted to a percentage by scaling between 120° and 180° with the equation: percentage alignment = (angle in degrees – 120) × (100/60).

Cell length and width were measured as described (Fernandez-Gonzalez and Zallen, 2011). A single ellipse was fitted to each cell. The lengths of the major and minor axes represent dorsal-ventral (DV) length and AP width, respectively. Oregon R was the wild-type control.

Junctional planar polarity was measured in SIESTA (Fernandez-Gonzalez and Zallen, 2011), a computational method developed in Matlab and DIPimage to calculate pixel intensities at cell edges. A straight line connecting the first and last pixel of each edge was used to determine its orientation. Background was the average of 20 cytoplasmic lines/image. A single ratio between the mean background-subtracted intensity for DV edges (0-45° relative to the AP axis) and AP edges (75-90° relative to the AP axis) was calculated for each embryo. An equal mix of Oregon R, *y w* and da-Gal4 embryos was the wild-type control.

For microtubule organization, each pixel was assigned an orientation and a value based on its intensity relative to its immediate surroundings (Chaudhuri et al., 1993) (R. Fernandez-Gonzalez and J.A.Z., unpublished). Pixel orientation was perpendicular to the gradient at that pixel; the gradient is a vector that points in the direction of the maximum local intensity change. Wild-type controls were embryos expressing *arm:GFP*, *sqh:GFP* or *resille:GFP* that were fixed and stained in the same tube.

Student's *t*-test was used for statistical comparisons between groups of wild-type and mutant embryos for edge alignment and denticle, junctional and microtubule localization; groups of wild-type and mutant cells for cell L:W ratios; and groups of wild-type and mutant denticle belts for edge growth and contraction.

RESULTS

Fat is required for the localization of actin-based denticle protrusions

Fat and Dachsous are required for denticle orientation in third-instar larvae (Repiso et al., 2010; Donoughe and DiNardo, 2011), but *dachsous* (*ds*) mutants have more restricted defects in the localization of denticle precursors in the embryo (Donoughe and DiNardo, 2011). To determine whether Fat is required for denticle organization in the *Drosophila* embryo, we analyzed embryos homozygous for the fat^{Grv} or fat^{NY1} null mutations. Each denticle belt contains six columns of actin-rich denticle precursors that initiate from the posterior cell cortex. In *fat* mutants, both denticle precursor placement and denticle orientation were disrupted in the posterior columns (Fig. 1A,B,L,M; supplementary material Fig. S1). Denticle precursors in columns 3-5 initiated from varying locations at the apical cortex, indicating a loss of planar polarity. By contrast, nearly all denticle precursors in column 6 initiated from the anterior cortex, suggesting a reversal of polarity in this column (Fig. 1B,M). Similar defects were observed in *ds* mutants, *fat ds* double mutants and embryos maternally and zygotically mutant for *fat* (Fig. 1C,D; supplementary material Fig. S1). Apical actin accumulated anteriorly at early stages in *fat* mutants (Fig. 1E,F), suggesting that Fat might direct the site of denticle precursor formation.

Although *frizzled* (*fz*) mutants have subtle denticle defects (Price et al., 2006), *fz* pathway mutations in third instar larvae enhance the denticle orientation defects in *ds* mutants (Casal et al., 2006; Donoughe and DiNardo, 2011). To investigate whether *fz* contributes to denticle precursor localization in the embryo, we generated embryos homozygous for fat^{Grv} and fz^{R52}. Denticle placement defects in column 3 were significantly enhanced in *fat; fz* double mutants, and the reversal of polarity in column 6 of *fat* mutants was converted to a more random distribution (Fig. 1B,H,L-

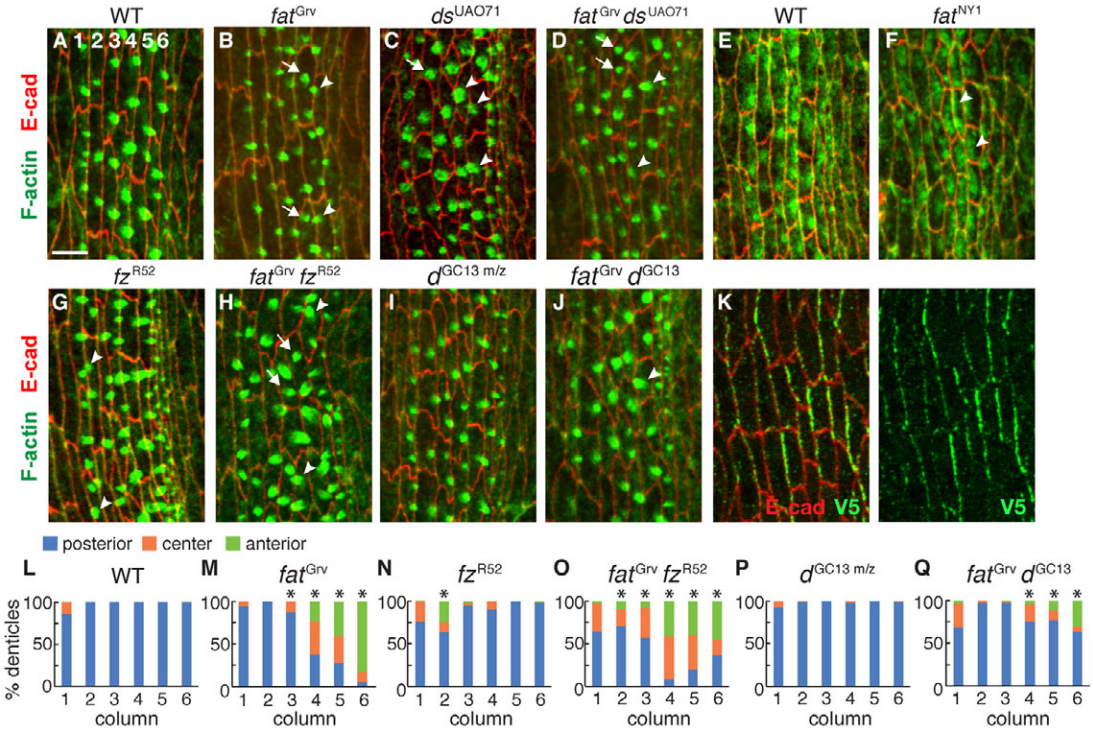

Fig. 1. Fat and Frizzled are differentially required for the localization of actin-based denticle protrusions. (**A-D**,**G-J**) Stage 15 denticle belts stained for F-actin (phalloidin, green) and E-cadherin (red) in *Drosophila* wild type (WT) (A), fat^{Grv} (B), ds^{UAO71} (C), fat^{Grv} ds^{UAO71} (D), fz^{R52} (G), fat^{Grv} fz^{R52} (H) and fat^{Grv} d^{GC13} (J) zygotic mutants and $d^{GC13\ m/z}$ embryos that lack maternal and zygotic *d* activity (I). Numbers indicate the denticle column. Examples of denticles that localize incorrectly to the anterior (arrowheads) or center (arrows) of the apical cortex are indicated. (**E**,**F**) Late stage 13 denticle belts in WT (E) and fat^{NY1} (F) stained for F-actin (phalloidin, green) and E-cadherin (red). Arrowheads indicate examples of anterior F-actin accumulation in fat^{NY1}. (**K**) Dachs:V5 is enriched at borders between anterior and posterior cells (AP edges). V5 (green), E-cadherin (red). Ventral views, anterior left. (**L-Q**) Percentage of denticle precursors at the posterior, center or anterior cell cortex in WT (L), fat^{Grv} (M), fz^{R52} (N), fat^{Grv} fz^{R52} (O), $d^{GC13\ m/z}$ (P) and fat^{Grv} d^{GC13} (Q). In column 3, 13% of denticles were misplaced in fat^{Grv} versus 44% in fat^{Grv} fz^{R52} (P<0.001). In column 4, 62% of denticles were misplaced in fat^{Grv} versus 91% in fat^{Grv} fz^{R52} (P=0.09). In column 6, 83% of denticles were anteriorly placed in fat^{Grv} versus 46% in fat^{Grv} fz^{R52} (P<0.02). 400-640 denticles were counted in four to six embryos/genotype. *P<0.05. Scale bar: 5 μm.

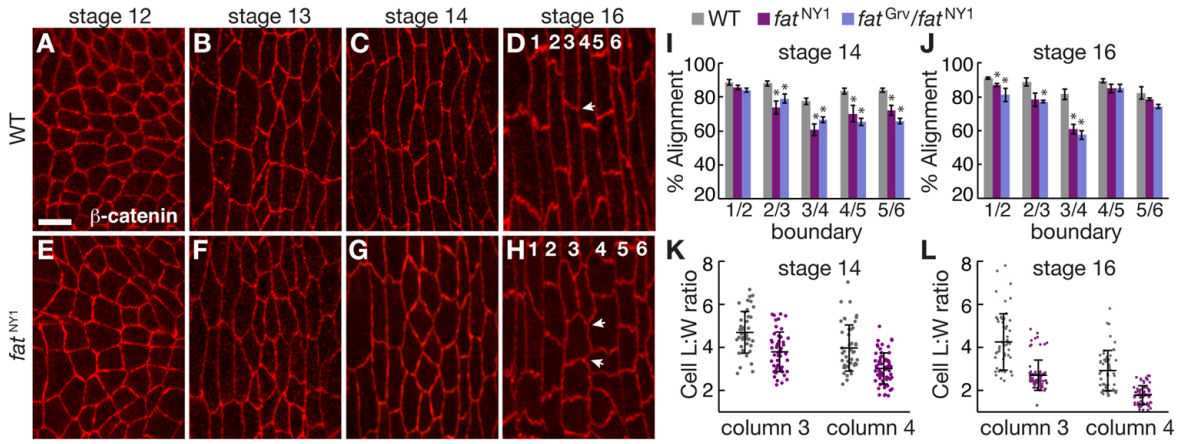

Fig. 2. Fat is required for cell shape in the denticle field. (**A-H**) Denticle belts stained for E-cadherin in *Drosophila* wild type (WT) (A-D) and *fat*^{NY1} (E-H). Arrows indicate angles between AP edges that are well aligned in WT (D) and poorly aligned in *fat* (H); numbers indicate the denticle column. Ventral views, anterior left. Scale bar: 5 μm. (**I**,**J**) Edge alignment in WT, *fat*^{NY1} and *fat*^{Grv}/*fat*^{NY1} at stages 14 (I) and 16 (J). At stage 14, alignment in *fat* mutants was reduced at the column 2/3 (P<0.05), 3/4 (P<0.01), 4/5 (P<0.05) and 5/6 boundaries (P<0.02). At stage 16, alignment in *fat* mutants was reduced at the column 1/2 (P<0.05) and 3/4 boundaries (P<0.01). A single value was obtained for each boundary in each embryo by averaging all angles for that boundary (40 angles in four embryos/boundary). The mean±s.e.m. of these values is shown. (**K**,**L**) Cell length:width (L:W) ratios (the ratio of cell length along the DV axis to cell width along the AP axis) in columns 3 and 4 of WT and *fat*^{NY1} at stages 14 (K) and 16 (L). Cell L:W ratios were decreased in *fat*^{NY1} compared with WT in columns 3 and 4 at both stages (P<0.001). A ratio was measured for each cell (43-56 cells in five embryos/column for WT, 49-75 cells in five embryos/column for *fat*^{NY1}). The mean (long black horizontal line) ± s.d. (black vertical line) of these values is shown. *P<0.05.

O). These results indicate that Fat and Frizzled both influence the planar polarized placement of denticle precursors in the embryo and suggest that Fat controls the direction of Frizzled signaling in the posterior denticle column.

The atypical myosin Dachs is an effector of Fat signaling (Mao et al., 2006; Rogulja et al., 2008). Expression of a tagged Dachs:V5 protein detected an asymmetric enrichment of Dachs at interfaces between anterior and posterior denticle cells (Fig. 1K). Denticle precursor placement defects were partially suppressed in *fat dachs* double mutants (Fig. 1J,Q). However, denticle precursors were correctly localized in embryos lacking maternal and zygotic *dachs* (Fig. 1I,P), suggesting that Dachs contributes to the denticle defects in *fat* mutants but does not play an essential role in this process.

Fat is required for planar polarized junctional remodeling

Prior to denticle formation, cells in the denticle field elongate parallel to the dorsal-ventral (DV) axis and align their anterior and posterior (AP) edges to form columns of rectangular-shaped cells (Fig. 2A-D) (Price et al., 2006; Walters et al., 2006; Simone and DiNardo, 2010). To determine whether Fat is required for these changes, we analyzed cell shape and behavior in *fat* mutants. Edge alignment was significantly reduced in *fat* mutants, with the strongest defects at the column 3/4 boundary (Fig. 2E-J). Using automated image analysis (Fernandez-Gonzalez and Zallen, 2011), we found that wild-type cells transition from a relatively isometric shape in stage 12 to become significantly elongated along the DV axis relative to their width along the AP axis at stage 16, achieving length:width (L:W) ratios of 4.3±0.2 in column 3 and 2.9±0.1 in column 4 (mean±s.e.m.; Fig. 2A,D,K,L). This elongation was significantly reduced in columns 2-5 of *fat*^{NY1} mutants, with L:W ratios of 2.7±0.08 in column 3 and 1.8±0.05 in column 4 at stage 16, 36% and 39% smaller than wild type, respectively (Fig. 2H,L; supplementary material Fig. S2). These results demonstrate that Fat is required for cell shape changes in the denticle field.

Cell rearrangements have been proposed to influence denticle cell shape (Simone and DiNardo, 2010). We therefore tested whether disrupted junctional remodeling could contribute to the defects in *fat* mutants. We performed time-lapse imaging from stage 13, 1 hour before the onset of denticle formation, until stage 16, when cuticle deposition begins. Most junctional remodeling events led to neighbor exchange in wild type (76%, n=183 cells in five embryos), whereas the remainder reformed the same edge, preserving the original cellular configuration (Fig. 3A-C). Cell boundaries were most dynamic in columns 3 and 4 in the center of the denticle field (Fig. 3D). These junctional remodeling events were planar polarized (Fig. 3E,F). Cell boundaries were primarily disassembled at interfaces between anterior and posterior cells (AP edges, 76% of shrinking edges, n=119) and new edges formed with a predominantly AP orientation (85% of forming edges, n=119). The frequency of junctional remodeling in *fat* mutants was similar to that observed in wild type (Fig. 3D). However, *fat* mutants had significantly increased growth and contraction of DV edges in column 3, such that AP and DV edges were equally active in *fat* mutants (Fig. 3E,F). Myosin II and F-actin localized correctly to the column 1/2 and 4/5 boundaries in *fat* mutants (supplementary material Fig. S3B,E), suggesting that Fat regulates cell shape through a mechanism distinct from localized actomyosin contractility. These results demonstrate that Fat is required for planar polarized junctional remodeling in the center of the denticle field, where cells are most dynamic in wild type.

Fat is required for the planar polarized localization of adherens junction proteins

Cell boundaries that display reduced edge growth and contraction in wild type have higher levels of adherens junction proteins (Colosimo and Tolwinski, 2006; Price et al., 2006; Kaplan and Tolwinski, 2010; Simone and DiNardo, 2010). To test whether excessive edge growth and contraction in *fat* mutants is due to a

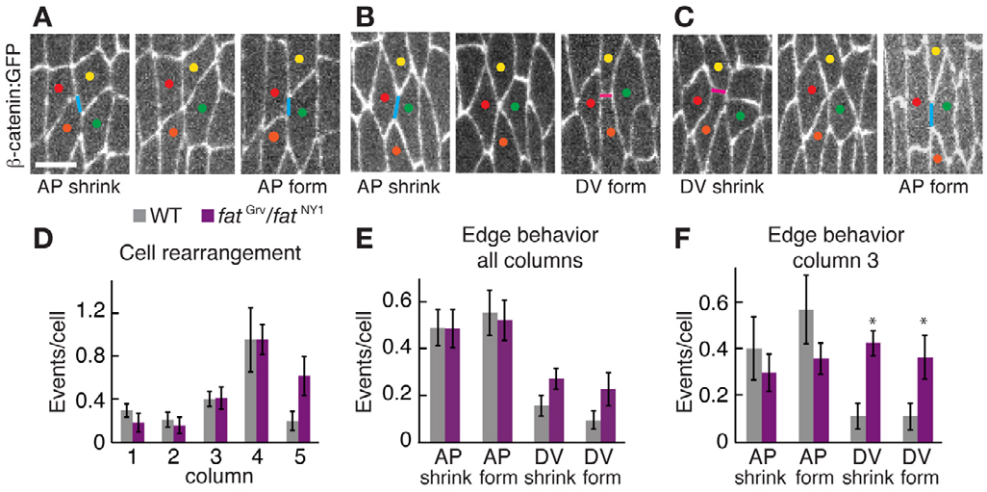

Fig. 3. Fat is required for planar polarized junctional remodeling. (**A-C**) Images from movies of wild-type (WT) *Drosophila* embryos expressing β-catenin:GFP. AP edges, blue lines; DV edges, pink lines. Colored dots mark individual cells. The three types of junctional remodeling leading to neighbor exchange are shown. (A) An AP edge between the yellow and orange cells shrinks and a new AP edge forms between the red and green cells (58% of neighbor exchange events, *n*=90). (B) An AP edge shrinks and a new DV edge forms (26% of neighbor exchange events). (C) A DV edge shrinks and a new AP edge forms (16% of neighbor exchange events). DV edges that shrink and form DV edges between new neighbors were not observed. Ventral views, anterior left. Scale bar: 5 μm. (**D**) Junctional remodeling events leading to cell rearrangement plotted by column in WT and fat^{Grv}/fat^{NY1} in stages 13-16. DV edges contacted cells of the same column; AP edges contacted cells posterior to a given column. There were no significant differences between WT and *fat*. (**E**) Junctional remodeling in all columns of WT and fat^{Grv}/fat^{NY1}. There were more shrinking AP edges than shrinking DV edges ($P<0.002$) and more forming AP edges than forming DV edges in WT ($P<0.001$). This bias was retained in *fat* mutants ($P=0.05$ for shrinking edges and $P=0.03$ for forming edges). (**F**) Junctional remodeling in column 3 of WT and fat^{Grv}/fat^{NY1}. *fat* mutants had more shrinking DV edges ($P<0.004$) and more forming DV edges ($P<0.03$) in column 3 compared with WT. No significant differences in AP edge behaviors were observed. A single value was obtained for each column in each denticle belt by normalizing the number of cell rearrangements to the number of cells (32-40 cells/column in nine denticle belts from five embryos for WT, 18-25 cells/column in five denticle belts from five embryos for $fat^{Grv/NY1}$). The mean ± s.e.m. of these values is shown. *$P<0.05$.

defect in junctional localization, we analyzed the distribution of adherens junction proteins. In wild type, β-catenin and the PDZ-domain proteins Baz (Par-3) and ZO-1 (Pyd) are strongly enriched at DV edges (Fig. 4A). Junctional planar polarity was first detected in stage 12 and increased over a period of 3 hours, reaching a maximum in stage 14 (Fig. 4D).

The planar polarized enrichment of junctional proteins at DV edges was significantly reduced in *fat* mutants, from a 2.7-fold enrichment of ZO-1 in wild type to 1.6-fold in fat^{NY1} (Fig. 4B,E). Similarly, Baz enrichment at DV edges was reduced from 4.1-fold in wild type to 2.1-fold in fat^{NY1}. In contrast to the denticle planar polarity defects, which were restricted to the posterior denticle columns, junctional planar polarity was reduced throughout the denticle field in *fat* mutants (Fig. 4F; data not shown). Because ZO-1, β-catenin and Baz accumulated to different extents in each column, we focused on column 3 to compare genotypes. Similar defects were observed in fat^{NY1} and embryos maternally and zygotically mutant for fat^{Grv} (Fig. 4E). Junctional planar polarity occurred normally in embryos maternally and zygotically mutant for *Van Gogh* (*Vang*), a component of the Frizzled planar cell polarity pathway, and *dachs*, an effector of Fat signaling, and junctional defects were partially suppressed in *fat dachs* double mutants (Fig. 4C,E; supplementary material Fig. S4). These results demonstrate that Fat is required for junctional planar polarity in the denticle field.

Junctional planar polarity requires Expanded, Hippo and Warts but is independent of Yorkie

In addition to its role in planar polarity, Fat is a tumor suppressor that regulates tissue growth by activating the Hippo/Warts kinase cascade (Bennett and Harvey, 2006; Cho et al., 2006; Hamaratoglu et al., 2006; Silva et al., 2006; Willecke et al., 2006; Tyler and Baker, 2007). Expanded, a component of this pathway, colocalizes with adherens junctions in denticle cells (supplementary material Fig. S5). To test whether Hippo/Warts signaling is required for planar polarity in the denticle field, we analyzed embryos maternally and zygotically mutant for *hippo* (*hpo*) or *warts* (*wts*) and embryos zygotically mutant for *expanded* (*ex*). Denticle precursors were correctly localized in *hippo* and *ex* mutants (supplementary material Fig. S6). However, *hippo*, *warts* and *ex* mutants displayed a significant reduction in junctional planar polarity (Fig. 5C-F,K). The fat^{Grv} ex^{E1} double mutant displayed junctional defects similar to the more severe single mutant (Fig. 5D,K), suggesting that Fat and Expanded might affect a common process. Cell elongation was reduced in *ex* and *hippo* mutants, but these defects were less severe than the defects in *fat* mutants (Fig. 5M). These results indicate that components of the Hippo/Warts pathway are required for junctional planar polarity.

In the absence of signaling by the cadherin Fat or the kinases Hippo and Warts, the transcriptional co-activator Yorkie localizes to the nucleus and drives the expression of genes that promote cell division and inhibit apoptosis (Huang et al., 2005; Reddy and Irvine, 2008; Badouel et al., 2009; Oh and Irvine, 2010). Phosphorylation of Yorkie by Warts excludes Yorkie from the nucleus (Dong et al., 2007; Zhao et al., 2007; Oh and Irvine, 2008). To investigate whether Fat regulates junctional polarity by inhibiting Yorkie, we expressed yki^{S168A}, an unphosphorylatable form of Yorkie that functions as a constitutively active protein (Oh and Irvine, 2008). We observed no effect on junctional localization in embryos that ectopically express yki^{S168A} (Fig. 5L). Conversely,

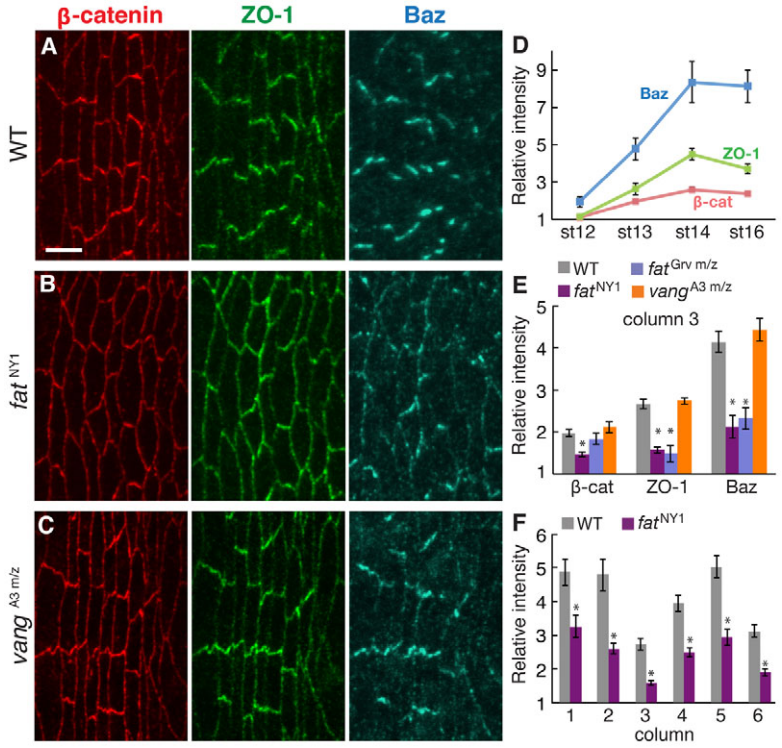

Fig. 4. Fat is required for the planar polarized localization of adherens junction proteins. (**A-C**) Stage 14 denticle belts stained for β-catenin (red), ZO-1 (green) and Baz (blue) in *Drosophila* wild type (WT) (A), *fat*^{NY1} (B) and embryos maternally and zygotically mutant for *vang*$^{A3\ m/z}$ (C). Ventral views, anterior left. Scale bar: 5 μm. (**D**) Enrichment of junctional proteins at DV edges (oriented at 0-45° relative to the AP axis) compared with AP edges (oriented at 75-90° relative to the AP axis) in all denticle columns in WT. (**E**) Enrichment of junctional proteins at DV edges in column 3 of stage 14 WT, *fat*^{NY1}, *fat*$^{Grv\ m/z}$ and *vang*$^{A3\ m/z}$ embryos. The planar polarized accumulation of junctional proteins was significantly reduced in *fat*^{NY1} (P<0.001 for β-catenin, ZO-1 and Baz) and *fat*$^{Grv\ m/z}$ (P<0.001 for ZO-1 and P<0.02 for Baz). (**F**) The enrichment of ZO-1 at DV edges was reduced in all columns of *fat*^{NY1} embryos at stage 14 (P<0.01 for column 1 and P<0.001 for columns 2-6). A single ratio between the mean DV and AP intensities was calculated for each embryo (five to seven cells in two denticle belts/embryo, three to 12 embryos for each stage and genotype). The mean ± s.e.m. of these values is shown. *P<0.05.

if loss of Fat leads to aberrant Yki activation, then removing Yki should suppress the defects in *fat* mutants. To test whether loss of Fat disrupts junctional localization by aberrantly activating Yki, we generated *fat* mutant embryos that were maternally and zygotically mutant for the *yki*^{B5} null allele. Embryos lacking *yki* had no obvious defects in junctional localization or cell shape (Fig. 5G,L,M). The *fat yki* double mutants had virtually no Yorkie protein by immunostaining (Fig. 5I,J), but displayed defects in junctional localization and cell shape comparable to *fat* mutants (Fig. 5H,L,M). These results demonstrate that Fat does not regulate junctional planar polarity by repressing Yorkie-mediated transcription.

Fat is required for planar polarized microtubule organization

Apical microtubules in the embryonic epithelium are preferentially oriented parallel to the DV axis (Fig. 6A,E) (Dickinson and Thatcher, 1997). We therefore investigated whether Fat could influence planar polarity by regulating microtubule organization. In *fat* mutants, microtubule alignment was preserved at the column 1/2 boundary, but microtubules in the remainder of the denticle field were highly disorganized (Fig. 6B,F). By contrast, microtubule alignment was not significantly affected in *ex* and *hippo* mutants (Fig. 6C,G). These results demonstrate that Fat is required for microtubule organization in denticle cells, which might contribute to the more severe defects in cell shape in *fat* mutants.

Microtubule orientation is evident throughout the ventral epidermis, both within the denticle belts and in the non-denticle-forming (smooth) cells between denticle belts (Dickinson and Thatcher, 1997). Smooth cells also display junctional planar polarity, although to a lesser extent than denticle cells. We found that microtubule and junctional planar polarity in smooth cells require Fat activity (the relative increase in α-tubulin signal oriented at 75-90° was 1.7±0.06 in wild type and 1.5±0.04 in *fat*^{NY1}, P=0.04; β-catenin enrichment at DV edges was 1.8±0.12 in wild type and 1.4±0.10 in *fat*^{NY1}, P=0.02, mean±s.e.m.), suggesting that Fat is required for planar polarity throughout the ventral epidermis. Smooth cells also elongate along the DV axis (L:W ratios of 2.9±0.8 at stage 14, mean±s.d.), but display differences in size and morphology compared with denticle cells. Further studies will be necessary to investigate the relationship between cell shape and planar polarity in different cell types.

Notch activation disrupts junctional planar polarity but not denticle localization

Defective growth pathway signaling is associated with an upregulation of Notch levels in the *Drosophila* wing disc (Maitra et al., 2006; Genevet et al., 2009), and the effects of *fat* or *ex* mutations on neuroepithelial differentiation resemble the effects of Notch activation (Reddy et al., 2010). We therefore wondered whether the defects in *fat* mutants could be due to altered Notch activity. Notch is expressed in the denticle field and we did not detect obvious defects in Notch localization or activity in *fat* mutants, although we cannot rule out subtle differences (supplementary material Fig. S7). To test whether Notch activation mimics the defects in *fat* mutants, we expressed the Notch intracellular domain (N^{intra}), which bypasses the requirement for proteolytic processing. Ectopic expression of N^{intra} has been shown to alter the pattern of gene expression in the denticle belt (Alexandre et al., 1999). We found that N^{intra} expression recapitulates several of the defects in *fat* mutants. First, the planar polarized distribution of β-catenin, ZO-1 and Baz was reduced in N^{intra}-expressing embryos (Fig. 7A-C). Second, microtubules were disorganized in N^{intra}-expressing embryos (Fig. 6D,H). Third, cell elongation and edge alignment were significantly reduced in N^{intra}-expressing embryos (Fig. 7D,E; supplementary material Fig. S7). Fourth, N^{intra}-expressing embryos displayed increased growth and contraction of DV edges in column 3 (Fig. 7F) and increased contraction of DV edges in column 4 (data not shown). N^{intra} expression disrupts neuroblast ingression and epithelial patterning,

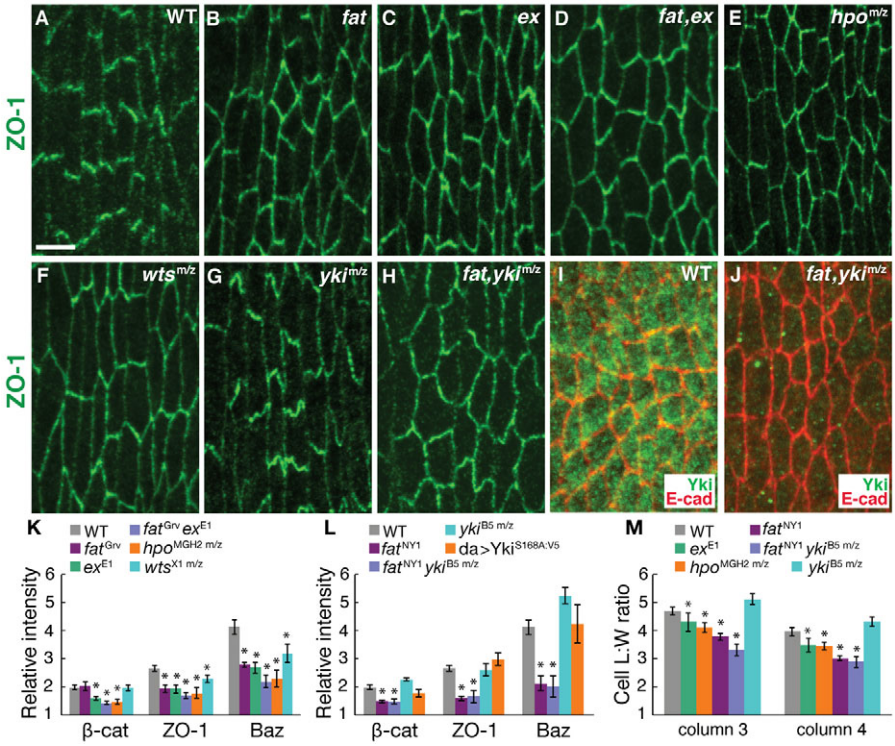

Fig. 5. Junctional planar polarity requires Expanded, Hippo and Warts but is independent of Yorkie. (**A-H**) Stage 14 denticle belts stained for ZO-1 (green) in *Drosophila* wild type (WT) (A); embryos zygotically mutant for fat^{Grv} (B), ex^{E1} (C), fat^{Grv} ex^{E1} (D); embryos maternally and zygotically mutant for $hpo^{MGH2\ m/z}$ (E), $wts^{X1\ m/z}$ (F), $yki^{B5\ m/z}$ (G); and embryos zygotically mutant for fat^{NY1} and maternally and zygotically mutant for yki^{B5} (fat^{NY1}, $yki^{B5\ m/z}$) (H). Ventral views, anterior left. Scale bar: 5 μm. (**I**,**J**) Stage 13 denticle belts stained for Yki (green) and E-cadherin (red) in WT (I) and fat^{NY1}, $yki^{B5\ m/z}$ (J). (**K**) Enrichment of junctional proteins at DV edges in column 3 of stage 14 embryos. The planar polarized accumulation of junctional proteins was reduced in *fat*, *ex*, *hpo* and *wts* ($P \leq 0.005$ for ZO-1 and Baz in fat^{Grv}; $P \leq 0.008$ for β-catenin, ZO-1 and Baz in ex^{E1}; $P \leq 0.005$ for β-catenin, ZO-1 and Baz in $hpo^{MGH2\ m/z}$; and $P=0.04$ for ZO-1 and Baz in $wts^{X1\ m/z}$). Junctional localization was not significantly different in fat^{Grv} ex^{E1} double mutants compared with ex^{E1} ($P=0.06$ for β-catenin; $P=0.2$ for ZO-1; $P=0.1$ for Baz). (**L**) Enrichment of junctional proteins at DV edges in column 3 of stage 14 embryos. fat^{NY1} $yki^{B5\ m/z}$ embryos displayed defects similar to fat^{NY1} ($P=0.9$ for β-catenin; $P=0.7$ for ZO-1; $P=0.8$ for Baz). A single ratio between the mean DV and AP intensities were calculated for each embryo (six to ten cells in two denticle belts/embryo, four to 12 embryos/genotype). The mean ± s.e.m. of these values is shown. (**M**) Cell length:width (L:W) ratios in columns 3 and 4 of stage 14 embryos. Cell L:W ratios were reduced in *ex*, *hpo*, *fat* and *fat yki* in both columns ($P<0.05$ for ex^{E1} and $hpo^{MGH2\ m/z}$; $P<0.001$ for fat^{NY1} and fat^{NY1} $yki^{B5\ m/z}$). A ratio was measured for each cell (31-56 cells per column in four to five embryos per genotype). The mean ± s.e.m. of these values is shown. *$P<0.05$.

and some embryos had extra denticle cells (supplementary material Fig. S6) (Alexandre et al., 1999). However, neuroblast ingression was not affected in *fat* mutants (5.7±2.8% of cells ingressed/hour in fat^{Grv}/fat^{NY1}, $n=644$ cells, versus 6.6±0.1% in wild type, $n=250$ cells), suggesting that the *fat* mutant defects are not secondary to defects in neuroblast ingression. Despite severe defects in cell shape, denticle precursor placement occurred normally in N^{intra}-expressing embryos (supplementary material Fig. S6). Together, these results demonstrate that Notch activation disrupts cell shape, junctional localization and microtubule organization in the denticle field, producing defects with striking similarities to the defects in *fat* mutants.

DISCUSSION

Fat regulates planar polarity in many cells and tissues, but the mechanisms by which Fat influences cell and tissue structure are not well understood. Here, we show that Fat is required for the localization of denticle actin precursors, microtubules and adherens junction proteins in the *Drosophila* embryo. Junctional remodeling in wild-type embryos is selectively suppressed at dorsal and ventral cell borders, which are sites of increased adherens junction accumulation. In *fat* mutants, decreased junctional planar polarity is associated with excessive growth and contraction at dorsal and ventral cell borders and a reduction in cell elongation and alignment. These results suggest a model in which Fat regulates planar polarized junctional localization and remodeling, which in turn influences cell shape. The atypical myosin Dachs is asymmetrically localized in denticle-forming cells and loss of *dachs* partially suppresses the denticle and junctional defects in *fat* mutants, suggesting that aberrant Dachs activity contributes to the defects in *fat* mutants. However, junctional and denticle planar polarity are correctly established in *dachs* mutants, indicating that Dachs is not essential for these processes. Defects in junctional planar polarity, but not denticle localization, are recapitulated in embryos that express activated Notch and embryos mutant for Expanded, Hippo or Warts. These results demonstrate an essential role for Fat and Hippo/Warts signaling in regulating planar polarized adherens junction localization in the *Drosophila* embryo.

Although the Hippo/Warts pathway has generally been thought to be separate from the role of Fat in planar polarity, we demonstrate an unexpected role for Expanded, Hippo and Warts in junctional planar polarity in the *Drosophila* embryo. Hippo/Warts signaling could influence planar polarity by modulating the size of the apical epithelial domain or the levels of junctional and signaling

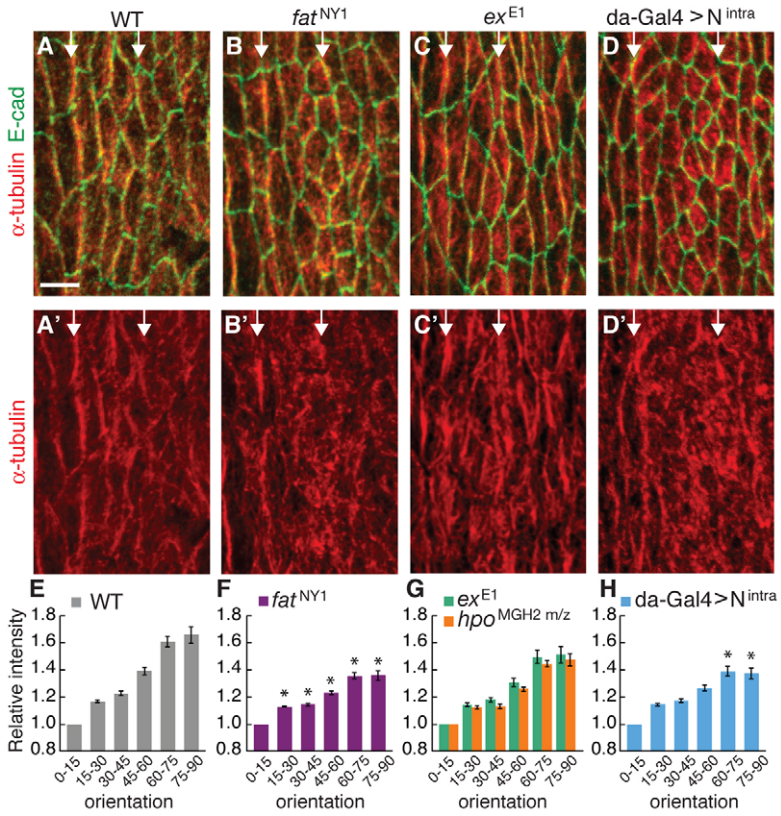

Fig. 6. Microtubule organization is disrupted in *fat* mutants. (**A-D'**) Stage 13 denticle belts stained for α-tubulin (red) and E-cadherin (green) in *Drosophila* wild type (WT) (A,A'), fat^{NY1} (B,B'), ex^{E1} (C,C') and da-Gal4 $>N^{intra}$ (D,D'). Arrows indicate column 1/2 and 4/5 boundaries. Ventral views, anterior left. Scale bar: 5 μm. (**E-H**) Microtubule orientation in stage 13 WT (E), embryos zygotically mutant for fat^{NY1} (F) or ex^{E1} (G), embryos maternally and zygotically mutant for $hpo^{MGH2\ m/z}$ (G) and da-Gal4 $>N^{intra}$ embryos (H). Orientation (*x*-axis) is the direction of the maximum local intensity difference for each pixel (0° parallel to and 90° perpendicular to the AP axis) and the relative intensity (*y*-axis) is the magnitude of this difference normalized to the 0-15° value. (E) WT α-tubulin signal was preferentially oriented perpendicular to the AP axis. (F) In fat^{NY1}, this orientational bias was significantly reduced ($P<0.01$ for all bins except 45-60°, $P=0.012$). (F) In da-Gal4 $>N^{intra}$, this orientational bias was reduced at 60-75° and 75-90° ($P<0.05$). A single value was obtained for each embryo by averaging two to three fields of eight to 25 cells (five to six embryos/genotype). The mean ± s.e.m. of these values is shown. *$P<0.05$.

proteins (Jaiswal et al., 2006; Maitra et al., 2006; Feng and Irvine, 2007; Genevet et al., 2009; Hamaratoglu et al., 2009) or by altering the expression of Four-jointed, a kinase that regulates the interaction between Fat and Ds (Cho et al., 2006; Ishikawa et al., 2008). However, these effects all require transcriptional activation by Yorkie. By contrast, the junctional defects in *fat* mutants are not suppressed by removing Yorkie or recapitulated by Yorkie activation, indicating that the role of Fat in planar polarity is independent of Yorkie-mediated transcription. Yorkie-independent effects of the Hippo/Warts pathway regulate dendrite maintenance (Emoto et al., 2006) and apical actin levels in epithelia (Fernández et al., 2011). These results raise the possibility that other effectors of Expanded, or other substrates of Warts, could mediate the effects of Fat on junctional planar polarity directly through signaling events at the cell cortex.

Junctional planar polarity in the denticle field is distinct from cytoskeletal planar polarity in several ways, suggesting that these processes involve different mechanisms of Fat signaling. Like hairs in the *Drosophila* wing (Zallen, 2007; Wu and Mlodzik, 2009; Goodrich and Strutt, 2011), denticles are unipolar structures that initiate from the posterior cell cortex (Colosimo and Tolwinski, 2006; Price et al., 2006; Walters et al., 2006). By contrast, adherens junctions are homophilic complexes that are likely to accumulate at both dorsal and ventral cell boundaries in a bipolar fashion. Second, denticle defects are specific to the posterior denticle belt in *fat* and *ds* mutants (Donoughe and DiNardo, 2011) (this work), whereas defects in cell shape, junctional localization and microtubule organization occur more broadly. Third, the placement of denticle actin precursors occurs normally, despite defects in cell shape and junctional localization, in activated Notch-expressing embryos and *ex*, *hippo* or *warts* mutants, demonstrating that these processes have distinct molecular requirements. In one model, Fat could regulate different processes by signaling through different effectors, with Ex, Hippo and Warts acting specifically in junctional regulation. Alternatively, Fat could influence different structures by acting at different locations in the cell. Further studies of the effectors required for the role of Fat in planar polarity will provide insight into the mechanisms by which Fat regulates multiple aspects of cellular organization.

The similar defects in *fat* mutants and embryos that express activated Notch suggest that Fat and Notch might affect a common process regulating cell shape and polarity. Activated Notch could disrupt cell shape and polarity indirectly, perhaps through changes in epidermal growth factor (EGF) receptor signaling (Alexandre et al., 1999; Wiellette and McGinnis, 1999; Walters et al., 2005; Maitra et al., 2006). Notch has been shown to be involved in morphogenetic processes such as compartment boundary formation in the *Drosophila* wing (Micchelli and Blair, 1999; Rauskolb et al., 1999), and an ectopic stripe of Notch is sufficient to induce cell alignment (Major and Irvine, 2005; Major and Irvine, 2006). Our results raise the possibility that Notch could influence cell morphology through its role in microtubule or junctional organization.

Here, we show that Fat is required for the organization of cells into aligned columns with discrete identities. Junctional remodeling in the denticle field is distinct from other examples of polarized cell behavior. During axis elongation in the *Drosophila* embryo, spatially regulated actomyosin contractility promotes junctional disassembly and inhibits junctional assembly at cell boundaries perpendicular to the axis of tissue elongation (Zallen and Wieschaus, 2004; Bertet et al., 2004; Blankenship et al., 2006). Despite a similar localization of myosin in the denticle field (Walters et al., 2006), most shrinking and growing edges share the same orientation. These results suggest a novel form of polarized

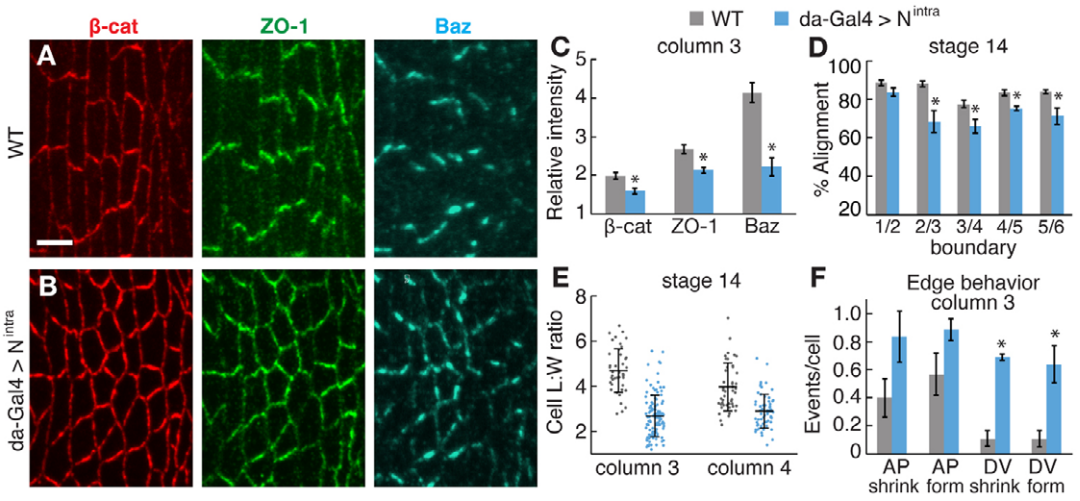

Fig. 7. Activated Notch disrupts cell shape and junctional planar polarity. (**A**,**B**) Stage 14 denticle belts stained for β-catenin (red), ZO-1 (green) and Baz (blue) in *Drosophila* wild type (WT) (A) and embryo expressing N^{intra} from the da-Gal4 driver (da-Gal4 >N^{intra}) (B). Ventral views, anterior left. Scale bar: 5 μm. (**C**) Enrichment of junctional proteins at DV edges in column 3 of stage 14 WT and da-Gal4 >N^{intra} embryos. Planar polarized junctional accumulation was reduced in da-Gal4 >N^{intra} (P=0.01 for β-catenin and ZO-1; P<0.001 for Baz). A single ratio between the mean DV and AP intensities was calculated for each embryo (six to seven cells in two denticle belts/embryo, five to 12 embryos/genotype). The mean ± s.e.m. of these values is shown. (**D**) Edge alignment in stage 14 embryos. Alignment in da-Gal4 >N^{intra} was reduced at column 2/3 (P<0.02), 3/4 (P<0.03), 4/5 (P<0.01) and 5/6 (P<0.03) boundaries. A single value was obtained for each boundary in each embryo by averaging all angles for that boundary (40 angles in four embryos/boundary). The mean ± s.e.m. of these values is shown. (**E**) Cell length:width (L:W) ratios in columns 3 and 4 of stage 14 WT and da-Gal4 >N^{intra} embryos. Cell L:W ratios were decreased in da-Gal4 >N^{intra} in both columns (P<0.0001). A ratio was obtained for each cell (40-50 cells/column in five embryos for WT; 40-100 cells/column in five embryos for da-Gal4 >N^{intra}). The mean (long black horizontal line) ± s.d. (black vertical line) of these values is shown. (**F**) AP and DV edge contraction and formation events per cell in column 3 of WT and da-Gal4 >N^{intra}. da-Gal4 >N^{intra} had more shrinking DV edges (P<0.001) and more forming DV edges (P=0.001) in column 3. No differences in AP edge behaviors were observed. A single value was obtained for each denticle belt by normalizing the number of cell rearrangements to the total number of cells (32-40 cells/column in nine denticle belts in five embryos for WT; 23-26 cells/column in four denticle belts in four embryos for da-Gal4 >N^{intra}). The mean ± s.e.m. of these values is shown. *P<0.05.

junctional remodeling in which junctional assembly and disassembly are activated in the same cellular domain, whereas other domains are largely quiescent. These behaviors could provide a mechanism that allows cells to maintain an unusual elongated, highly aligned configuration by continually exerting tension on each other's boundaries, resulting in an inevitable degree of edge growth and contraction. Our results suggest that in addition to polarized actomyosin contractility (Walters et al., 2006; Simone and DiNardo, 2010), junctional remodeling must be actively suppressed at dorsal and ventral cell boundaries in a Fat-dependent mechanism that is necessary for cell shape and tissue organization. This mechanism may be generally relevant to other structures that form during compartment boundary formation (Major and Irvine, 2006; Landsberg et al., 2009; Monier et al., 2010), ectoderm segmentation (Browne et al., 2005; Hannibal et al., 2012), and lens and retinal cells in the vertebrate eye (Nowak et al., 2009; Kwan et al., 2012; Salbreux et al., 2012). Fat/Dachsous signaling is required for polarized cell division and cell rearrangements in *Drosophila* (Baena-López et al., 2005; Aigouy et al., 2010; Bosveld et al., 2012), and for tissue elongation in the mouse neural tube, cochlea, kidney and intestines (Saburi et al., 2008; Saburi et al., 2012; Mao et al., 2011a). The ability of Fat to regulate junctional remodeling and cytoskeletal polarity may be important for its diverse roles in tissue organization.

Acknowledgements
We are grateful to Rodrigo Fernandez-Gonzalez and Dene Farrell for computational methods; and Nick Baker, Hilary Ellis, Rick Fehon, Iswar Hariharan, Kieran Harvey, Ken Irvine, Gary Struhl and the Bloomington *Drosophila* stock center at Indiana University for fly stocks and antibodies. We thank Rodrigo Fernandez-Gonzalez, Karen Kasza, Marina Soares e Silva, Sergio Simoes, Alison Spencer, Masako Tamada and Athea Vichas for comments on the manuscript.

Funding
This work was supported by a W. M. Keck Foundation Distinguished Young Scholar in Medical Research Award to J.A.Z. J.A.Z. is an Early Career Scientist of the Howard Hughes Medical Institute. Deposited in PMC for release after 6 months.

Competing interests statement
The authors declare no competing financial interests.

Supplementary material
Supplementary material available online at
http://dev.biologists.org/lookup/suppl/doi:10.1242/dev.083949/-/DC1

References
Adler, P. N., Charlton, J., Jones, K. H. and Liu, J. (1994). The cold-sensitive period for frizzled in the development of wing hair polarity ends prior to the start of hair morphogenesis. *Mech. Dev.* **46**, 101-107.
Adler, P. N., Charlton, J. and Liu, J. (1998). Mutations in the cadherin superfamily member gene dachsous cause a tissue polarity phenotype by altering frizzled signaling. *Development* **125**, 959-968.
Aigouy, B., Farhadifar, R., Staple, D. B., Sagner, A., Röper, J. C., Jülicher, F. and Eaton, S. (2010). Cell flow reorients the axis of planar polarity in the wing epithelium of Drosophila. *Cell* **142**, 773-786.
Alexandre, C., Lecourtois, M. and Vincent, J.-P. (1999). Wingless and Hedgehog pattern Drosophila denticle belts by regulating the production of short-range signals. *Development* **126**, 5689-5698.
Ambegaonkar, A. A., Pan, G., Mani, M., Feng, Y. and Irvine, K. D. (2012). Propagation of Dachsous-Fat planar cell polarity. *Curr. Biol.* **22**, 1302-1308.
Badouel, C., Gardano, L., Amin, N., Garg, A., Rosenfeld, R., Le Bihan, T. and McNeill, H. (2009). The FERM-domain protein Expanded regulates Hippo

pathway activity via direct interactions with the transcriptional activator Yorkie. *Dev. Cell* **16**, 411-420.
Baena-López, L. A., Baonza, A. and García-Bellido, A. (2005). The orientation of cell divisions determines the shape of Drosophila organs. *Curr. Biol.* **15**, 1640-1644.
Bate, M. and Martinez Arias, A. (1993). *The Development of Drosophila melanogaster*. Plainview, NY: Cold Spring Harbor Laboratory Press.
Bennett, F. C. and Harvey, K. F. (2006). Fat cadherin modulates organ size in Drosophila via the Salvador/Warts/Hippo signaling pathway. *Curr. Biol.* **16**, 2101-2110.
Bertet, C., Sulak, L. and Lecuit, T. (2004). Myosin-dependent junction remodelling controls planar cell intercalation and axis elongation. *Nature* **429**, 667-671.
Blankenship, J. T., Backovic, S. T., Sanny, J. S., Weitz, O. and Zallen, J. A. (2006). Multicellular rosette formation links planar cell polarity to tissue morphogenesis. *Dev. Cell* **11**, 459-470.
Boedigheimer, M. and Laughon, A. (1993). Expanded: a gene involved in the control of cell proliferation in imaginal discs. *Development* **118**, 1291-1301.
Bosveld, F., Bonnet, I., Guirao, B., Tlili, S., Wang, Z., Petitalot, A., Marchand, R., Bardet, P. L., Marcq, P., Graner, F. et al. (2012). Mechanical control of morphogenesis by Fat/Dachsous/Four-jointed planar cell polarity pathway. *Science* **336**, 724-727.
Brittle, A., Thomas, C. and Strutt, D. (2012). Planar polarity specification through asymmetric subcellular localization of Fat and Dachsous. *Curr. Biol.* **22**, 907-914.
Browne, W. E., Price, A. L., Gerberding, M. and Patel, N. H. (2005). Stages of embryonic development in the amphipod crustacean, Parhyale hawaiensis. *Genesis* **42**, 124-149.
Bryant, P. J., Huettner, B., Held, L. I. J., Jr, Ryerse, J. and Szidonya, J. (1988). Mutations at the fat locus interfere with cell proliferation control and epithelial morphogenesis in Drosophila. *Dev. Biol.* **129**, 541-554.
Casal, J., Struhl, G. and Lawrence, P. A. (2002). Developmental compartments and planar polarity in Drosophila. *Curr. Biol.* **12**, 1189-1198.
Casal, J., Lawrence, P. A. and Struhl, G. (2006). Two separate molecular systems, Dachsous/Fat and Starry night/Frizzled, act independently to confer planar cell polarity. *Development* **133**, 4561-4572.
Chaudhuri, B. B., Kundu, K. and Sarkar, N. (1993). Detection and gradation of oriented texture. *Pattern Recognit. Lett.* **14**, 147-153.
Cho, E., Feng, Y., Rauskolb, C., Maitra, S., Fehon, R. and Irvine, K. D. (2006). Delineation of a Fat tumor suppressor pathway. *Nat. Genet.* **38**, 1142-1150.
Chou, T. B. and Perrimon, N. (1996). The autosomal FLP-DFS technique for generating germline mosaics in Drosophila melanogaster. *Genetics* **144**, 1673-1679.
Colosimo, P. F. and Tolwinski, N. S. (2006). Wnt, Hedgehog and junctional Armadillo/beta-catenin establish planar polarity in the Drosophila embryo. *PLoS ONE* **1**, e9.
Dickinson, W. J. and Thatcher, J. W. (1997). Morphogenesis of denticles and hairs in Drosophila embryos: involvement of actin-associated proteins that also affect adult structures. *Cell Motil. Cytoskeleton* **38**, 9-21.
Dong, J., Feldmann, G., Huang, J., Wu, S., Zhang, N., Comerford, S. A., Gayyed, M. F., Anders, R. A., Maitra, A. and Pan, D. (2007). Elucidation of a universal size-control mechanism in Drosophila and mammals. *Cell* **130**, 1120-1133.
Donoughe, S. and DiNardo, S. (2011). dachsous and frizzled contribute separately to planar polarity in the Drosophila ventral epidermis. *Development* **138**, 2751-2759.
Emoto, K., Parrish, J. Z., Jan, L. Y. and Jan, Y. N. (2006). The tumour suppressor Hippo acts with the NDR kinases in dendritic tiling and maintenance. *Nature* **443**, 210-213.
Fanto, M., Clayton, L., Meredith, J., Hardiman, K., Charroux, B., Kerridge, S. and McNeill, H. (2003). The tumor-suppressor and cell adhesion molecule Fat controls planar polarity via physical interactions with Atrophin, a transcriptional co-repressor. *Development* **130**, 763-774.
Feng, Y. and Irvine, K. D. (2007). Fat and expanded act in parallel to regulate growth through warts. *Proc. Natl. Acad. Sci. USA* **104**, 20362-20367.
Fernández, B. G., Gaspar, P., Brás-Pereira, C., Jezowska, B., Rebelo, S. R. and Janody, F. (2011). Actin-Capping Protein and the Hippo pathway regulate F-actin and tissue growth in Drosophila. *Development* **138**, 2337-2346.
Fernandez-Gonzalez, R. and Zallen, J. A. (2011). Oscillatory behaviors and hierarchical assembly of contractile structures in intercalating cells. *Phys. Biol.* **8**, 045005.
Genevet, A., Polesello, C., Blight, K., Robertson, F., Collinson, L. M., Pichaud, F. and Tapon, N. (2009). The Hippo pathway regulates apical-domain size independently of its growth-control function. *J. Cell Sci.* **122**, 2360-2370.
Go, M. J., Eastman, D. S. and Artavanis-Tsakonas, S. (1998). Cell proliferation control by Notch signaling in Drosophila development. *Development* **125**, 2031-2040.
Goetz, S. C. and Anderson, K. V. (2010). The primary cilium: a signalling centre during vertebrate development. *Nat. Rev. Genet.* **11**, 331-344.
Goodrich, L. V. and Strutt, D. (2011). Principles of planar polarity in animal development. *Development* **138**, 1877-1892.
Gray, R. S., Roszko, I. and Solnica-Krezel, L. (2011). Planar cell polarity: coordinating morphogenetic cell behaviors with embryonic polarity. *Dev. Cell* **21**, 120-133.
Hamaratoglu, F., Willecke, M., Kango-Singh, M., Nolo, R., Hyun, E., Tao, C., Jafar-Nejad, H. and Halder, G. (2006). The tumour-suppressor genes NF2/Merlin and Expanded act through Hippo signalling to regulate cell proliferation and apoptosis. *Nat. Cell Biol.* **8**, 27-36.
Hamaratoglu, F., Gajewski, K., Sansores-Garcia, L., Morrison, C., Tao, C. and Halder, G. (2009). The Hippo tumor-suppressor pathway regulates apical-domain size in parallel to tissue growth. *J. Cell Sci.* **122**, 2351-2359.
Hannibal, R. L., Price, A. L. and Patel, N. H. (2012). The functional relationship between ectodermal and mesodermal segmentation in the crustacean, Parhyale hawaiensis. *Dev. Biol.* **361**, 427-438.
Harumoto, T., Ito, M., Shimada, Y., Kobayashi, T. J., Ueda, H. R., Lu, B. and Uemura, T. (2010). Atypical cadherins Dachsous and Fat control dynamics of noncentrosomal microtubules in planar cell polarity. *Dev. Cell* **19**, 389-401.
Harvey, K. F., Pfleger, C. M. and Hariharan, I. K. (2003). The Drosophila Mst ortholog, hippo, restricts growth and cell proliferation and promotes apoptosis. *Cell* **114**, 457-467.
Hashimoto, M. and Hamada, H. (2010). Translation of anterior-posterior polarity into left-right polarity in the mouse embryo. *Curr. Opin. Genet. Dev.* **20**, 433-437.
Huang, J., Wu, S., Barrera, J., Matthews, K. and Pan, D. (2005). The Hippo signaling pathway coordinately regulates cell proliferation and apoptosis by inactivating Yorkie, the Drosophila Homolog of YAP. *Cell* **122**, 421-434.
Ishikawa, H. O., Takeuchi, H., Haltiwanger, R. S. and Irvine, K. D. (2008). Four-jointed is a Golgi kinase that phosphorylates a subset of cadherin domains. *Science* **321**, 401-404.
Jaiswal, M., Agrawal, N. and Sinha, P. (2006). Fat and Wingless signaling oppositely regulate epithelial cell-cell adhesion and distal wing development in Drosophila. *Development* **133**, 925-935.
Kaplan, N. A. and Tolwinski, N. S. (2010). Spatially defined Dsh-Lgl interaction contributes to directional tissue morphogenesis. *J. Cell Sci.* **123**, 3157-3165.
Kelly, M. C. and Chen, P. (2009). Development of form and function in the mammalian cochlea. *Curr. Opin. Neurobiol.* **19**, 395-401.
Kwan, K. M., Otsuna, H., Kidokoro, H., Carney, K. R., Saijoh, Y. and Chien, C. B. (2012). A complex choreography of cell movements shapes the vertebrate eye. *Development* **139**, 359-372.
Landsberg, K. P., Farhadifar, R., Ranft, J., Umetsu, D., Widmann, T. J., Bittig, T., Said, A., Jülicher, F. and Dahmann, C. (2009). Increased cell bond tension governs cell sorting at the Drosophila anteroposterior compartment boundary. *Curr. Biol.* **19**, 1950-1955.
Ma, D., Yang, C. H., McNeill, H., Simon, M. A. and Axelrod, J. D. (2003). Fidelity in planar cell polarity signalling. *Nature* **421**, 543-547.
Maitra, S., Kulikauskas, R. M., Gavilan, H. and Fehon, R. G. (2006). The tumor suppressors Merlin and Expanded function cooperatively to modulate receptor endocytosis and signaling. *Curr. Biol.* **16**, 702-709.
Major, R. J. and Irvine, K. D. (2005). Influence of Notch on dorsoventral compartmentalization and actin organization in the Drosophila wing. *Development* **132**, 3823-3833.
Major, R. J. and Irvine, K. D. (2006). Localization and requirement for Myosin II at the dorsal-ventral compartment boundary of the Drosophila wing. *Dev. Dyn.* **235**, 3051-3058.
Mao, Y., Rauskolb, C., Cho, E., Hu, W. L., Hayter, H., Minihan, G., Katz, F. N. and Irvine, K. D. (2006). Dachs: an unconventional myosin that functions downstream of Fat to regulate growth, affinity and gene expression in Drosophila. *Development* **133**, 2539-2551.
Mao, Y., Mulvaney, J., Zakaria, S., Yu, T., Morgan, K. M., Allen, S., Basson, M. A., Francis-West, P. and Irvine, K. D. (2011a). Characterization of a Dchs1 mutant mouse reveals requirements for Dchs1-Fat4 signaling during mammalian development. *Development* **138**, 947-957.
Mao, Y., Tournier, A. L., Bates, P. A., Gale, J. E., Tapon, N. and Thompson, B. J. (2011b). Planar polarization of the atypical myosin Dachs orients cell divisions in Drosophila. *Genes Dev.* **25**, 131-136.
Marshall, W. F. and Kintner, C. (2008). Cilia orientation and the fluid mechanics of development. *Curr. Opin. Cell Biol.* **20**, 48-52.
Matakatsu, H. and Blair, S. S. (2004). Interactions between Fat and Dachsous and the regulation of planar cell polarity in the Drosophila wing. *Development* **131**, 3785-3794.
Matakatsu, H. and Blair, S. S. (2006). Separating the adhesive and signaling functions of the Fat and Dachsous protocadherins. *Development* **133**, 2315-2324.
Matakatsu, H. and Blair, S. S. (2012). Separating planar cell polarity and Hippo pathway activities of the protocadherins Fat and Dachsous. *Development* **139**, 1498-1508.
McCartney, B. M., McEwen, D. G., Grevengoed, E., Maddox, P., Bejsovec, A. and Peifer, M. (2001). Drosophila APC2 and Armadillo participate in tethering mitotic spindles to cortical actin. *Nat. Cell Biol.* **3**, 933-938.

Micchelli, C. A. and Blair, S. S. (1999). Dorsoventral lineage restriction in wing imaginal discs requires Notch. *Nature* **401**, 473-476.
Monier, B., Pélissier-Monier, A., Brand, A. H. and Sanson, B. (2010). An actomyosin-based barrier inhibits cell mixing at compartmental boundaries in Drosophila embryos. *Nat. Cell Biol.* **12**, 60-65, 1-9.
Nowak, R. B., Fischer, R. S., Zoltoski, R. K., Kuszak, J. R. and Fowler, V. M. (2009). Tropomodulin1 is required for membrane skeleton organization and hexagonal geometry of fiber cells in the mouse lens. *J. Cell Biol.* **186**, 915-928.
Oh, H. and Irvine, K. D. (2008). In vivo regulation of Yorkie phosphorylation and localization. *Development* **135**, 1081-1088.
Oh, H. and Irvine, K. D. (2010). Yorkie: the final destination of Hippo signaling. *Trends Cell Biol.* **20**, 410-417.
Pellock, B. J., Buff, E., White, K. and Hariharan, I. K. (2007). The Drosophila tumor suppressors Expanded and Merlin differentially regulate cell cycle exit, apoptosis, and Wingless signaling. *Dev. Biol.* **304**, 102-115.
Price, M. H., Roberts, D. M., McCartney, B. M., Jezuit, E. and Peifer, M. (2006). Cytoskeletal dynamics and cell signaling during planar polarity establishment in the *Drosophila* embryonic denticle. *J. Cell Sci.* **119**, 403-415.
Rauskolb, C., Correia, T. and Irvine, K. D. (1999). Fringe-dependent separation of dorsal and ventral cells in the Drosophila wing. *Nature* **401**, 476-480.
Reddy, B. V. and Irvine, K. D. (2008). The Fat and Warts signaling pathways: new insights into their regulation, mechanism and conservation. *Development* **135**, 2827-2838.
Reddy, B. V., Rauskolb, C. and Irvine, K. D. (2010). Influence of fat-hippo and notch signaling on the proliferation and differentiation of Drosophila optic neuroepithelia. *Development* **137**, 2397-2408.
Repiso, A., Saavedra, P., Casal, J. and Lawrence, P. A. (2010). Planar cell polarity: the orientation of larval denticles in Drosophila appears to depend on gradients of Dachsous and Fat. *Development* **137**, 3411-3415.
Rogulja, D., Rauskolb, C. and Irvine, K. D. (2008). Morphogen control of wing growth through the Fat signaling pathway. *Dev. Cell* **15**, 309-321.
Saburi, S., Hester, I., Fischer, E., Pontoglio, M., Eremina, V., Gessler, M., Quaggin, S. E., Harrison, R., Mount, R. and McNeill, H. (2008). Loss of Fat4 disrupts PCP signaling and oriented cell division and leads to cystic kidney disease. *Nat. Genet.* **40**, 1010-1015.
Saburi, S., Hester, I., Goodrich, L. and McNeill, H. (2012). Functional interactions between Fat family cadherins in tissue morphogenesis and planar polarity. *Development* **139**, 1806-1820.
Salbreux, G., Barthel, L. K., Raymond, P. A. and Lubensky, D. K. (2012). Coupling mechanical deformations and planar cell polarity to create regular patterns in the zebrafish retina. *PLoS Comput. Biol.* **8**, e1002618.
Shimada, Y., Yonemura, S., Ohkura, H., Strutt, D. and Uemura, T. (2006). Polarized transport of Frizzled along the planar microtubule arrays in Drosophila wing epithelium. *Dev. Cell* **10**, 209-222.
Silva, E., Tsatskis, Y., Gardano, L., Tapon, N. and McNeill, H. (2006). The tumor-suppressor gene fat controls tissue growth upstream of expanded in the hippo signaling pathway. *Curr. Biol.* **16**, 2081-2089.
Simon, M. A. (2004). Planar cell polarity in the Drosophila eye is directed by graded Four-jointed and Dachsous expression. *Development* **131**, 6175-6184.
Simone, R. P. and DiNardo, S. (2010). Actomyosin contractility and Discs large contribute to junctional conversion in guiding cell alignment within the Drosophila embryonic epithelium. *Development* **137**, 1385-1394.
Struhl, G. and Adachi, A. (1998). Nuclear access and action of notch in vivo. *Cell* **93**, 649-660.
Strutt, H. and Strutt, D. (2002). Nonautonomous planar polarity patterning in Drosophila: dishevelled-independent functions of frizzled. *Dev. Cell* **3**, 851-863.
Taylor, J., Abramova, N., Charlton, J. and Adler, P. N. (1998). Van Gogh: a new Drosophila tissue polarity gene. *Genetics* **150**, 199-210.
Thomas, C. and Strutt, D. (2012). The roles of the cadherins Fat and Dachsous in planar polarity specification in Drosophila. *Dev. Dyn.* **241**, 27-39.
Tyler, D. M. and Baker, N. E. (2007). Expanded and fat regulate growth and differentiation in the Drosophila eye through multiple signaling pathways. *Dev. Biol.* **305**, 187-201.
Tyler, D. M., Li, W., Zhuo, N., Pellock, B. and Baker, N. E. (2007). Genes affecting cell competition in Drosophila. *Genetics* **175**, 643-657.
Wallingford, J. B. (2010). Planar cell polarity signaling, cilia and polarized ciliary beating. *Curr. Opin. Cell Biol.* **22**, 597-604.
Walters, J. W., Muñoz, C., Paaby, A. B. and DiNardo, S. (2005). Serrate-Notch signaling defines the scope of the initial denticle field by modulating EGFR activation. *Dev. Biol.* **286**, 415-426.
Walters, J. W., Dilks, S. A. and DiNardo, S. (2006). Planar polarization of the denticle field in the Drosophila embryo: roles for Myosin II (zipper) and fringe. *Dev. Biol.* **297**, 323-339.
Wei, X. and Ellis, H. M. (2001). Localization of the Drosophila MAGUK protein Polychaetoid is controlled by alternative splicing. *Mech. Dev.* **100**, 217-231.
Wiellette, E. L. and McGinnis, W. (1999). Hox genes differentially regulate Serrate to generate segment-specific structures. *Development* **126**, 1985-1995.
Willecke, M., Hamaratoglu, F., Kango-Singh, M., Udan, R., Chen, C. L., Tao, C., Zhang, X. and Halder, G. (2006). The fat cadherin acts through the hippo tumor-suppressor pathway to regulate tissue size. *Curr. Biol.* **16**, 2090-2100.
Wu, J. and Mlodzik, M. (2009). A quest for the mechanism regulating global planar cell polarity of tissues. *Trends Cell Biol.* **19**, 295-305.
Xu, T., Wang, W., Zhang, S., Stewart, R. A. and Yu, W. (1995). Identifying tumor suppressors in genetic mosaics: the Drosophila lats gene encodes a putative protein kinase. *Development* **121**, 1053-1063.
Yang, C. H., Axelrod, J. D. and Simon, M. A. (2002). Regulation of Frizzled by fat-like cadherins during planar polarity signaling in the Drosophila compound eye. *Cell* **108**, 675-688.
Zallen, J. A. (2007). Planar polarity and tissue morphogenesis. *Cell* **129**, 1051-1063.
Zallen, J. A. and Wieschaus, E. (2004). Patterned gene expression directs bipolar planar polarity in Drosophila. *Dev. Cell* **6**, 343-355.
Zeidler, M. P., Perrimon, N. and Strutt, D. I. (1999). The four-jointed gene is required in the Drosophila eye for ommatidial polarity specification. *Curr. Biol.* **9**, 1363-1372.
Zeidler, M. P., Perrimon, N. and Strutt, D. I. (2000). Multiple roles for four-jointed in planar polarity and limb patterning. *Dev. Biol.* **228**, 181-196.
Zhang, S., Xu, L., Lee, J. and Xu, T. (2002). Drosophila atrophin homolog functions as a transcriptional corepressor in multiple developmental processes. *Cell* **108**, 45-56.
Zhao, B., Wei, X., Li, W., Udan, R. S., Yang, Q., Kim, J., Xie, J., Ikenoue, T., Yu, J., Li, L. et al. (2007). Inactivation of YAP oncoprotein by the Hippo pathway is involved in cell contact inhibition and tissue growth control. *Genes Dev.* **21**, 2747-2761.

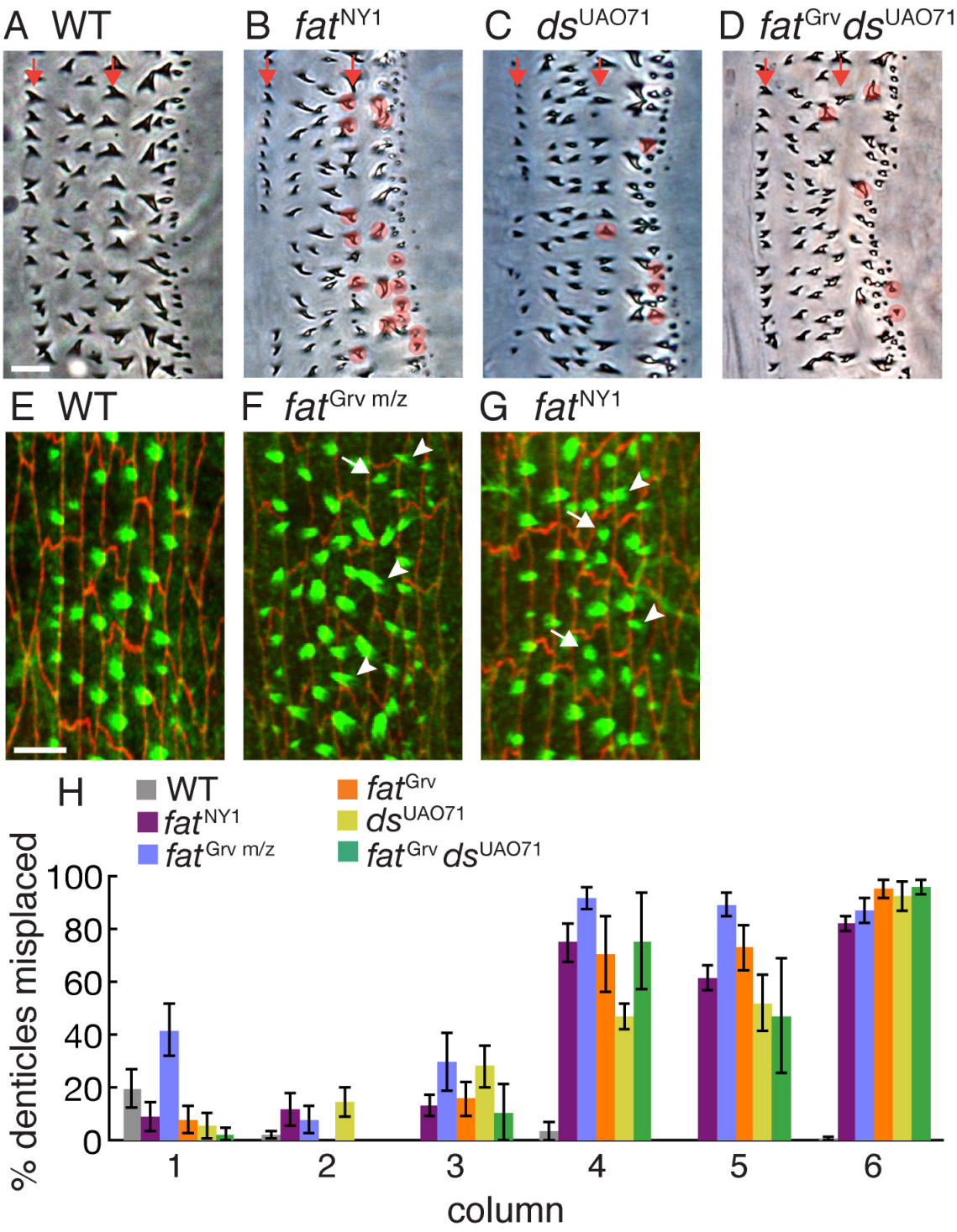

Fig. S1. Denticle placement defects in *fat* and *dachsous* mutants. (**A-D**) Cuticle preparations of wild-type (WT) (A), *fat*^{NY1} (B), *ds*^{UAO71} (C) and *fat*^{Grv} *ds*^{UAO71} (D) embryos. A majority of denticles point posteriorly in WT, with the exception of columns 1 and 4 (arrows), which point anteriorly. Misoriented denticles are highlighted in red. (**E-G**) Stage 15 denticle belts stained for F-actin (phalloidin, green) and E-cadherin (red) in WT (E), *fat*$^{Grv\ m/z}$ mutants that lack maternal and zygotic *fat* activity (F) and *fat*^{NY1} zygotic mutants (G). Ventral views, anterior left. (**H**) Percentage of misplaced denticle precursors by column in WT, *fat*^{NY1} zygotic mutants, *fat*$^{Grv\ m/z}$ mutants, *fat*^{Grv} zygotic mutants, *ds*^{UA071} zygotic mutants and *fat*^{Grv} *ds*^{UA071} double zygotic mutants. All mutants were significantly different from WT in columns 4-6 (P<0.01). All mutant genotypes except *fat*^{Grv} *ds*^{UA071} were significantly different from WT in column 3 (P<0.05). Denticle placement defects in embryos lacking maternal and zygotic *fat*^{Grv} activity were not significantly different from *fat*^{Grv} zygotic mutants except in column 1 (P=0.008). A single value was obtained for each column in each embryo (400-640 denticles in four to six embryos/genotype). The mean±s.e.m. of these values is shown. Scale bars: 5 μm.

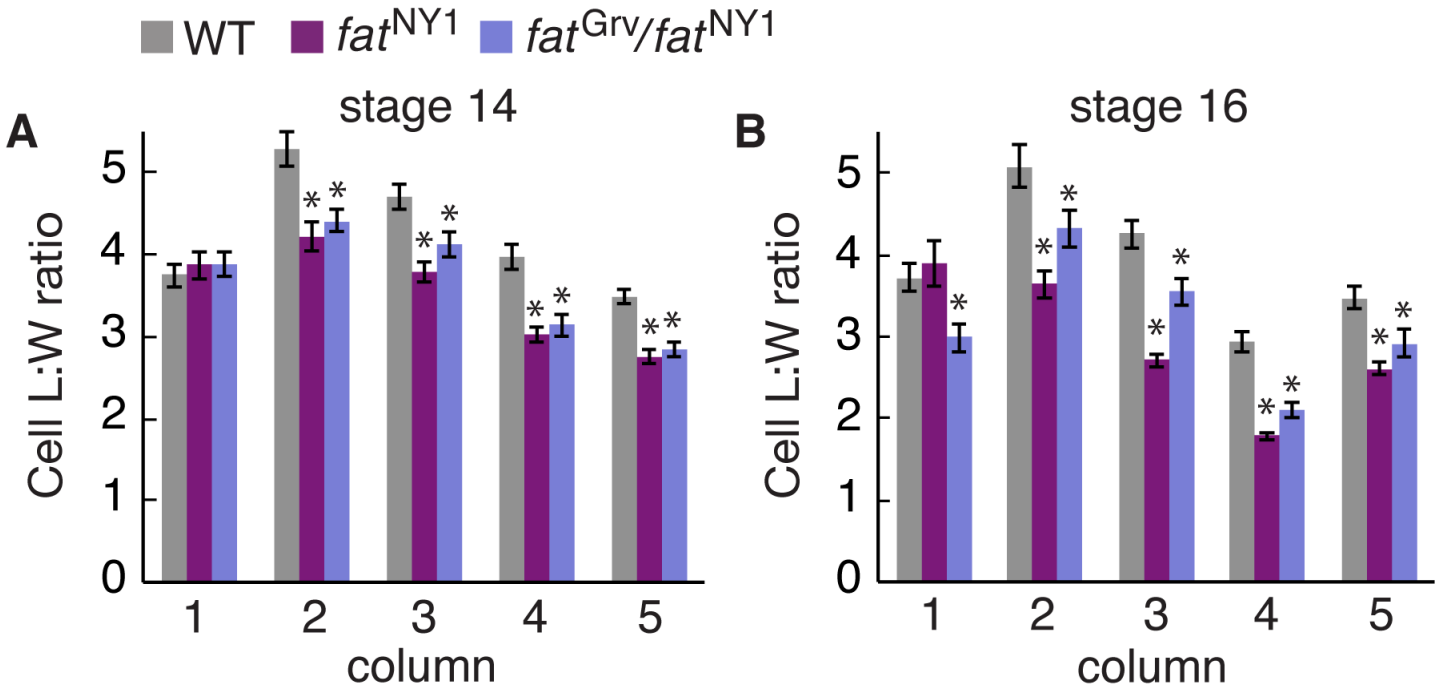

Fig. S2. Cell shape defects in *fat* mutants. Cell length:width (L:W) ratios (the ratio of cell length along the DV axis to cell width along the AP axis) plotted by column in stage 14 wild type (WT), *fat*^{NY1} zygotic mutant and *fat*^{Grv}/*fat*^{NY1} transheterozygous embryos. (**A**) Stage 14 cell L:W ratios were decreased in *fat*^{NY1} in columns 2-5 (P<0.001), and in *fat*^{Grv}/*fat*^{NY1} in columns 2 (P<0.001), 3 (P=0.01), 4 (P<0.001) and 5 (P<0.001). (**B**) Stage 16 cell L:W ratios were decreased in *fat*^{NY1} in columns 2-5 (P<0.001) and in *fat*^{Grv}/*fat*^{NY1} in columns 1 (P<0.01), 2(P<0.05), 3 (P<0.01), 4 (P<0.001) and 5 (P=0.012). A ratio was measured for each cell (40-75 cells in four embryos/column). The mean±s.e.m. of these values is shown. Asterisks indicate statistical significance.

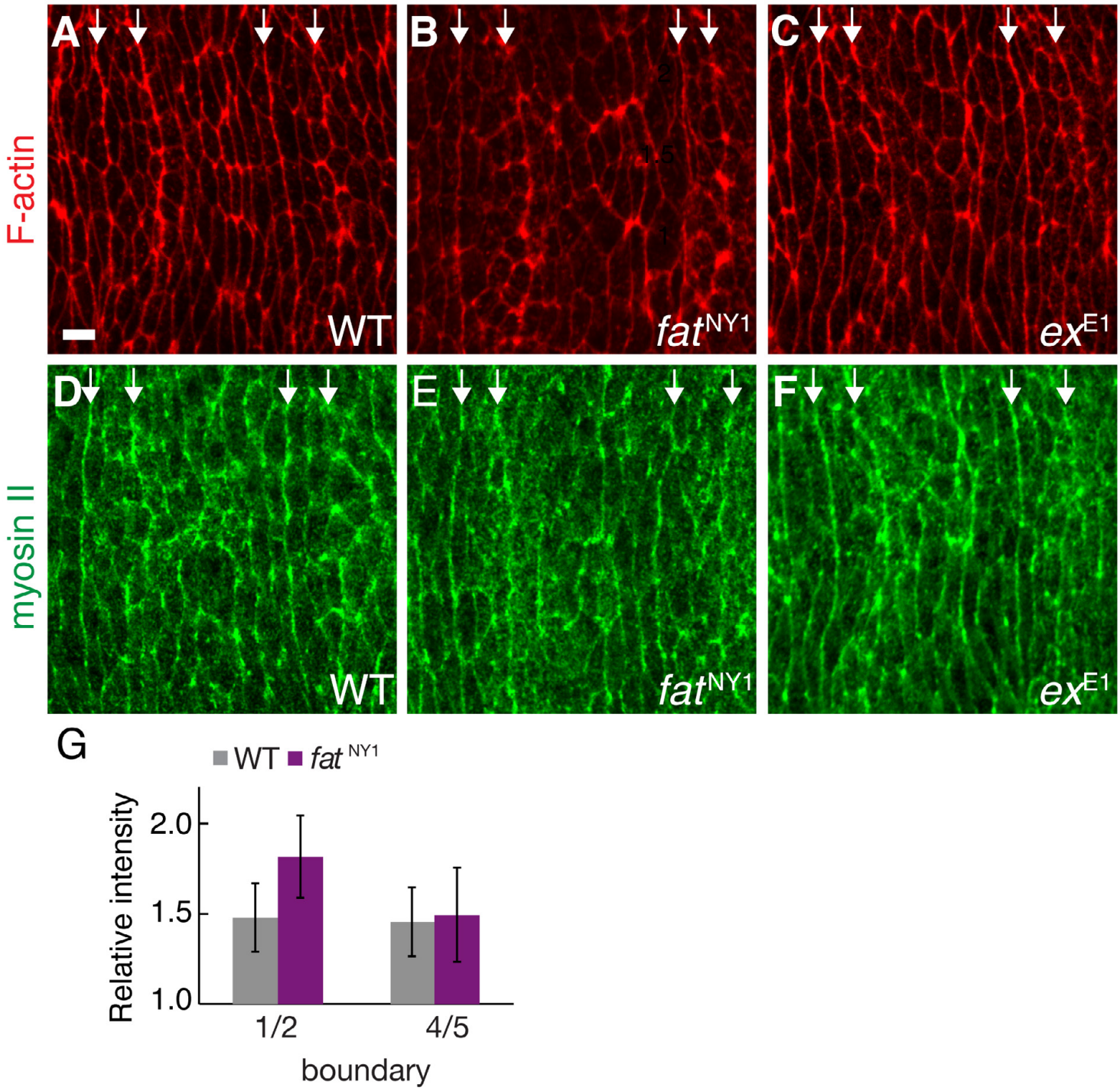

Fig. S3. Myosin and F-actin are correctly enriched at specific column boundaries in *fat* mutants. (**A-C**) Mid-stage 13 denticle belts in wild type (WT) (A), *fat*^{NY1} (B) and *ex*^{E1} (C) embryos stained with phalloidin to visualize F-actin. (**D-F**) Mid-stage 13 denticle belts in WT (D), *fat*^{NY1} (E) and *ex*^{E1} (F) embryos expressing a myosin II regulatory light chain GFP fusion (sqh:GFP) visualized with antibodies to GFP. Myosin II and F-actin accumulate at the column 1/2 and 4/5 boundaries (arrows) to a similar extent in WT, *fat* and *ex*. Ventral views, anterior left. (**G**) Enrichment of myosin II at AP edges compared with DV edges at the column 1/2 and 4/5 boundaries in WT and *fat*^{NY1}. In WT, myosin was enriched 1.5±0.2-fold at the column 1/2 boundary and 1.5±0.2-fold at the column 4/5 boundary. In *fat*^{NY1}, myosin was enriched 1.8±0.2-fold at the column 1/2 boundary and 1.5±0.3-fold at the column 4/5 boundary. A single value was obtained for each embryo by averaging the ratio of the average AP intensity to the average DV intensity for six to seven cells in two denticle belts/embryo (three to four embryos/genotype). The mean±s.e.m. of these values is shown. Scale bar: 5 μm.

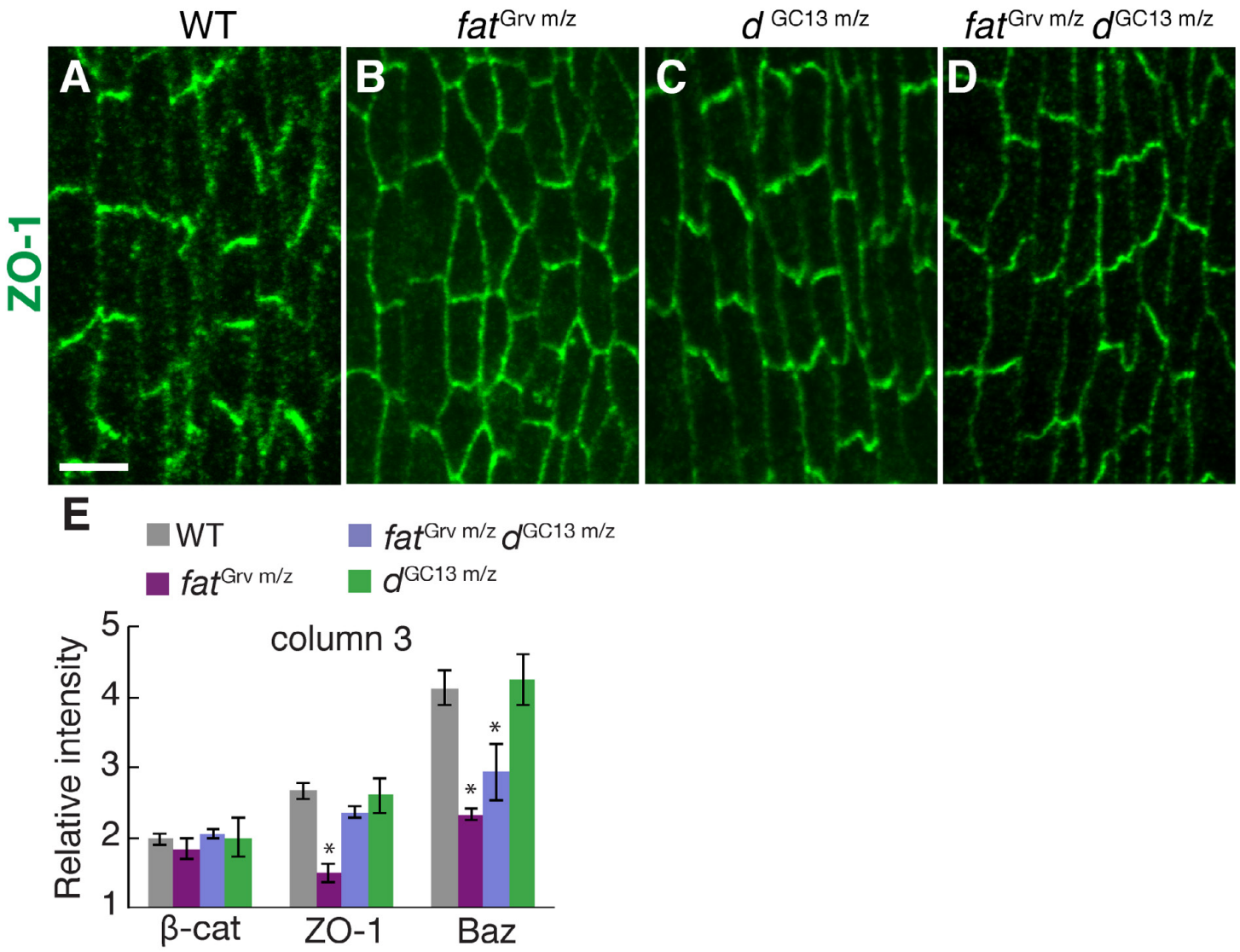

Fig. S4. Loss of *dachs* suppresses a subset of the junctional defects in *fat* mutants. (**A-D**) Stage 14 denticle belts stained for ZO-1 (green) in wild type (WT) (A) and embryos maternally and zygotically mutant for $fat^{Grv\ m/z}$ (B), $d^{GC13\ m/z}$ (C) and both $fat^{Grv\ m/z}$ and $d^{GC13\ m/z}$ (D). Scale bar: 5 μm. (**E**) Enrichment of junctional proteins at DV edges in column 3 of stage 14 embryos of the indicated genotypes. The enrichment of ZO-1 and Baz was significantly reduced in $fat^{Grv\ m/z}$ ($P<0.001$ for ZO-1 and $P<0.02$ for Baz). $d^{GC13\ m/z}$ was not significantly different from WT. Embryos doubly mutant for *fat* and *dachs* had WT ZO-1 localization ($P=0.2$ compared with WT, $P=0.04$ compared with $fat^{Grv\ m/z}$). However, Baz enrichment was significantly reduced in *fat dachs* double mutants ($P=0.02$ compared with WT), indicating that *dachs* does not suppress all aspects of the *fat* mutant phenotype. A single value was calculated for each embryo by measuring the ratio of average DV intensity to average AP intensity for five to seven cells in two denticle belts/embryo; $n=4$ embryos for each genotype. The mean±s.e.m. of these values is shown.

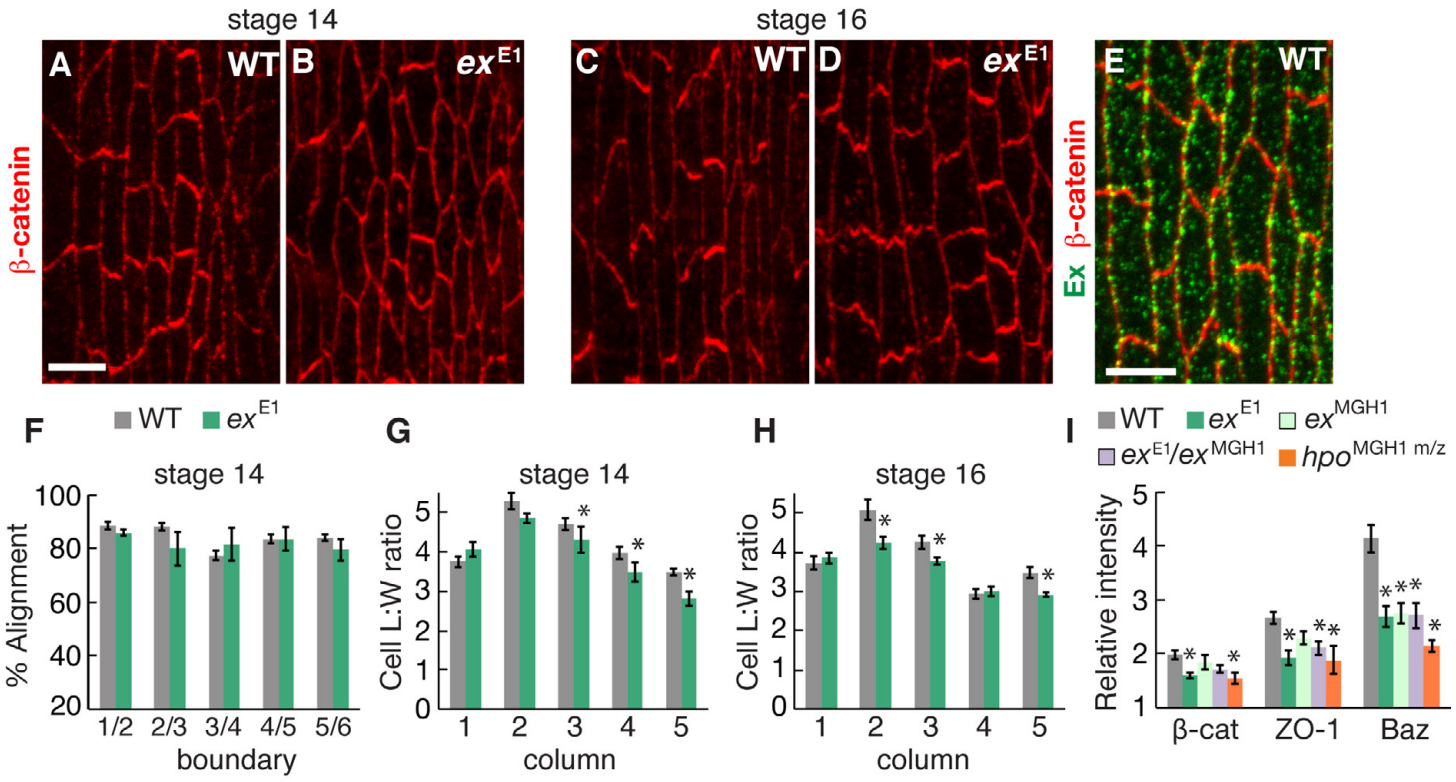

Fig. S5. Cell-shape defects in *expanded* mutants. (**A-D**) Denticle belts stained for β-catenin in wild type (WT) (A,C) and ex^{E1} (B,D) embryos at stage 14 (A,B) or stage 16 (C,D). Ventral views, anterior left. Scale bar: 5 μm. (**E**) WT denticle belt stained for Ex (green) and β-catenin (red) at stage 14. (**F**) Edge alignment in WT (gray) and ex^{E1} (green) at stage 14. Alignment in ex^{E1} was not significantly different from WT. A single value was obtained for each column boundary in each embryo by averaging all angles measured for that boundary (40 angles in four embryos/boundary). The mean±s.e.m. of these values is shown. (**G**,**H**) Cell length:width (L:W) ratios (the ratio of cell length along the DV axis to cell width along the AP axis) plotted by column in WT and ex^{E1} at stage 14 (G) and stage 16 (H). Cell L:W ratios were decreased in stage 14 ex^{E1} embryos compared with WT in columns 3 (P=0.02), 4 (P=0.04) and 5 (P<0.001), and in stage 16 ex^{E1} embryos in columns 2 (P=0.006), 3 (P=0.01) and 5 (P<0.001). A ratio was measured for each cell (30-75 cells in four embryos/column). The mean±s.e.m. of these values is shown. (**I**) Enrichment of junctional proteins at DV edges in column 3 of stage 14 WT, ex^{E1}, ex^{MGH1}, ex^{E1}/ex^{MGH1} and $hpo^{MGH1\ m/z}$ embryos. The enrichment of several junctional proteins at DV edges was significantly reduced in ex^{E1} (P<0.001 for β-catenin, ZO-1 and Baz), ex^{MGH1} (P=0.005 for Baz), ex^{E1}/ex^{MGH1} (P=0.04 for ZO-1; P=0.02 for Baz) and $hpo^{MGH1\ m/z}$ (P<0.02 for β-cat; P=0.006 for ZO-1; and P<0.001 for Baz). A single value was calculated for each embryo by measuring the ratio of the average DV intensity to the average AP intensity for five to seven cells in two denticle belts/embryo; n=4 embryos for each genotype. The mean±s.e.m. of these values is shown. Maternal gene products may obscure additional requirements for Ex, as we were unable to obtain embryos that lack maternal *ex* activity.

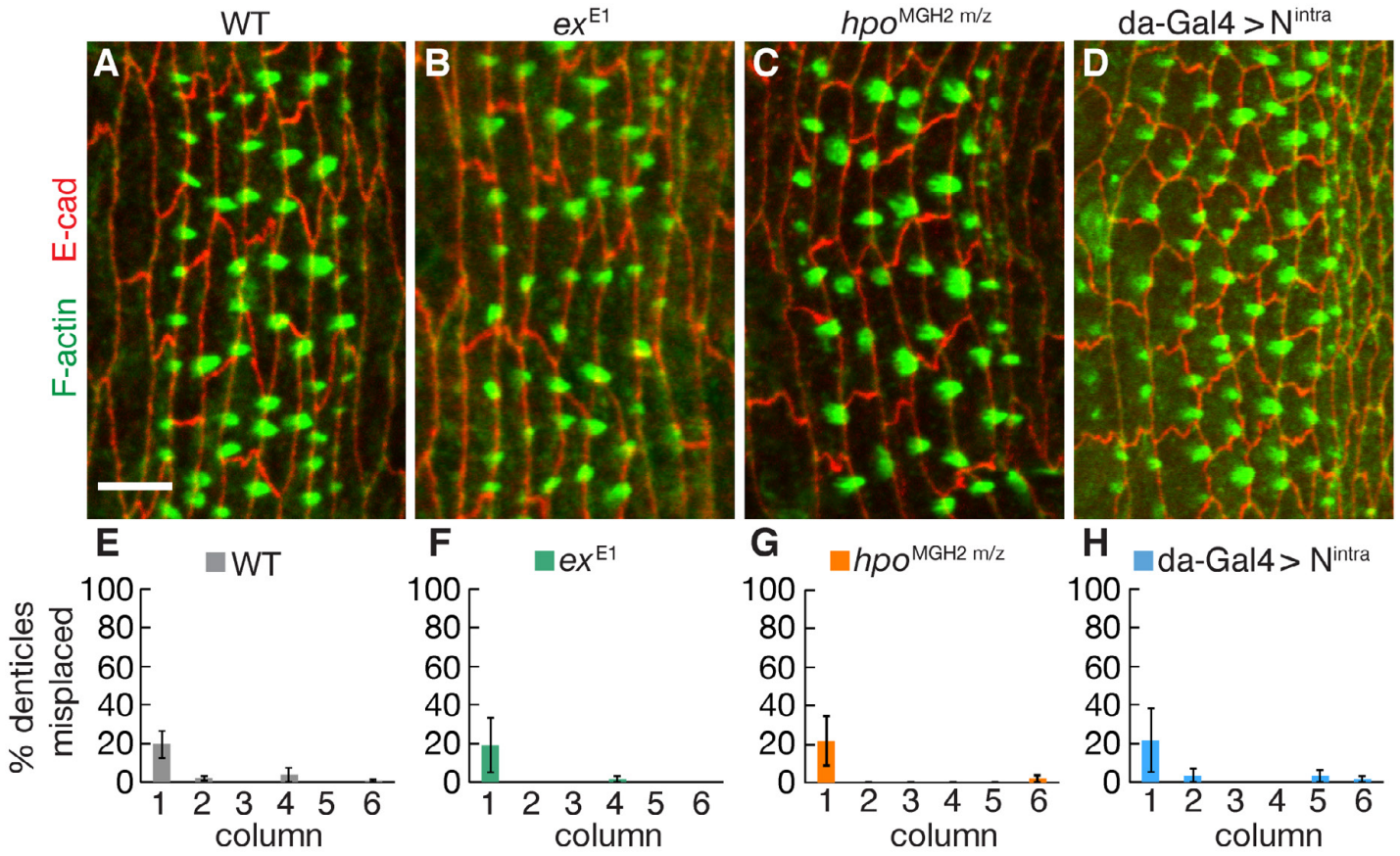

Fig. S6. Denticle placement in wild-type, *ex* mutant and N^{intra}-expressing embryos. (**A-D**) Stage 15 denticle belts stained for F-actin (phalloidin, green) and E-cadherin (red) in wild type (WT) (A), *ex*^{E1} (B), *hpo*$^{MGH2\ m/z}$ (C) and da-Gal4>N^{intra} (D) embryos. Scale bar: 5 μm. (**E-H**) Percentage of misplaced denticle precursors plotted by column for WT (E), *ex*^{E1} (F), *hpo*$^{MGH2\ m/z}$ (G) and da-Gal4>N^{intra} (H) embryos. Denticle precursors were correctly localized to the posterior cell cortex. Ventral views, anterior left. A single value was obtained for each column in each embryo (354-464 denticles in three to five embryos/genotype). The mean±s.e.m. of these values is shown.

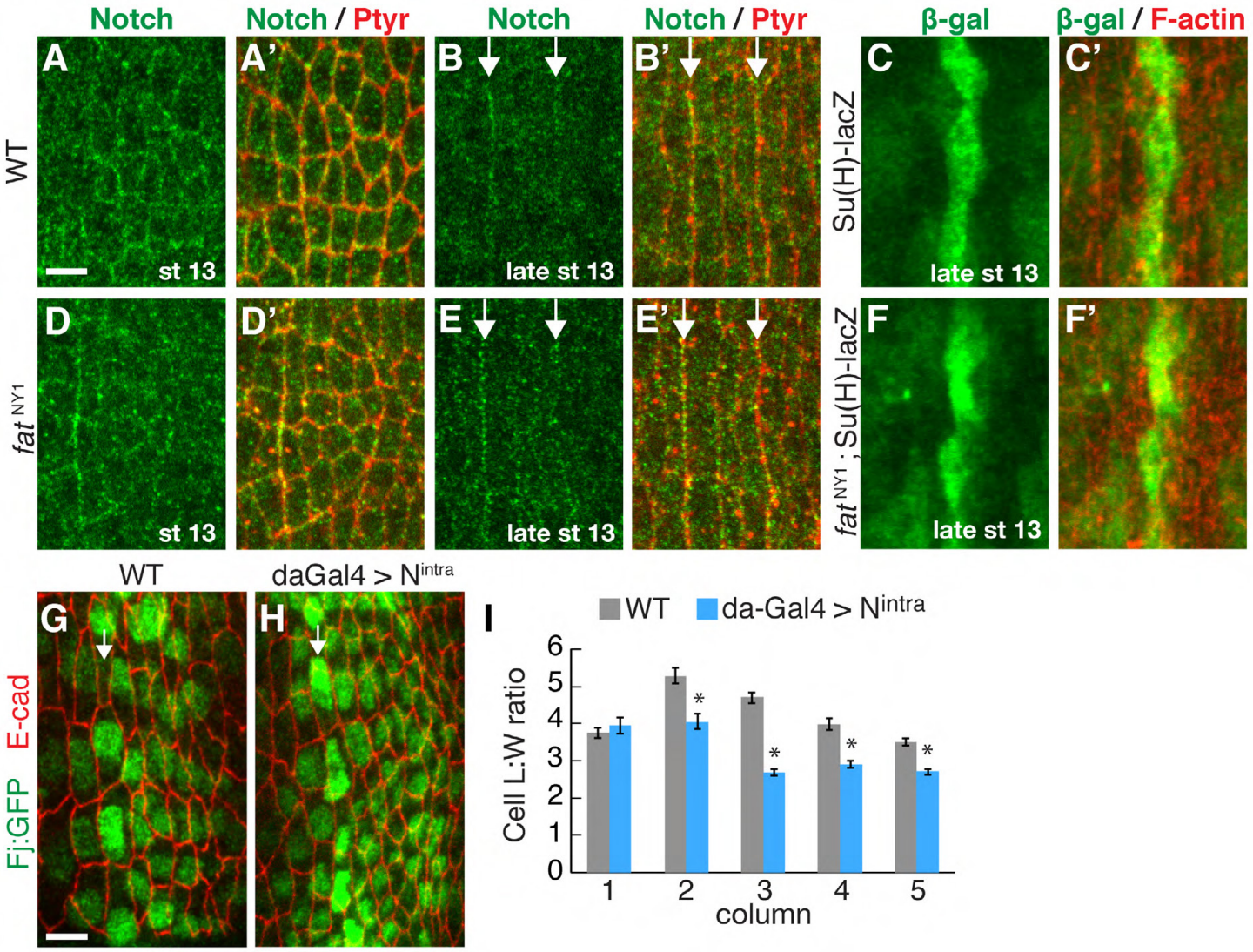

Fig. S7. Notch activation recapitulates the cell-shape defects of *fat* mutants. (**A-B′**,**D-E′**) Denticle belts at the indicated stages stained for Notch (green) and phosphotyrosine (Ptyr, red). (A,D) In early stage 13, Notch localizes to the apical cortex of wild-type (WT) (A) and *fat*^{NY1} (D) embryos. (B) In late stage 13, Notch is enriched at the column 1/2 and 4/5 boundaries (arrows) in WT. (E) This localization occurs normally in *fat*^{NY1}. (**C**,**F**) Late stage 13 denticle belts stained for F-actin (phalloidin, red) and β-gal (green) to visualize the expression of the Su(H)*lacZ* Notch activity reporter in WT (C) and *fat*^{NY1} (F). The column 4-specific pattern of Su(H)*lacZ* expression occurs normally in *fat*^{NY1}. Ventral views, anterior left. (**G**,**H**) Localization of the endogenous Four-jointed protein using a Four-jointed:GFP (Fj:GFP) trap line visualized with antibodies to GFP. Fj:GFP was expressed throughout the denticle field, with an enrichment in column 2 (arrows). This enrichment of Fj:GFP expression was retained in N^{intra}-expressing embryos, although a broadening of the Fj domain is apparent. (**I**) Cell length:width (L:W) ratios (the ratio of cell length along the DV axis to cell width along the AP axis) plotted by column in stage 14 WT and da-Gal4>N^{intra} embryos. Cell L:W ratios were decreased in da-Gal4>N^{intra} compared with WT in columns 2-5 (P<0.001). A ratio was measured for each cell (40-100 cells in four embryos/column). The mean±s.e.m. of these values is shown. Scale bars: 5 μm.